The Carbon Skeleton of the Belt Region of Fullerene C_{84} (D_2)

Wolf Dietrich Neudorff,*[a] Dieter Lentz,[b] Maribel Anibarro,[b] and A. Dieter Schlüter*[a]

Abstract: The synthesis and structural characterization of the double-stranded carbon skeleton in the belt region of a C_{84} fullerene has been achieved. The synthetic methodology used is based on cyclic dimerization of diastereomeric AB-type monomers **18** by a non-diastereospecific Diels–Alder reaction with isobenzofuran and acenaphthylene groups as reactive termini. Four diasteromeric monomer precursors **17** were prepared for the first time by the use of dihydropyracylene (**12**) in a multistep synthesis. The synthesis of dihydropyracylene itself has been optimized to the degree that it is now available on the 10 g scale. The belt-shaped macrocycle **19**, obtained from dimerization of the monomers **17**, could be partly aromatized by an acid-catalyzed dehydration reaction to give **23**, which differs from the fully unsaturated belt by two "water" molecules. Semiempirical AM1 calculations of the electronic and thermodynamic properties of cyclic fluoranthenes revealed strain energy as the essential reason for the incomplete aromatization of **19**. The structures of the macrocycles **19** and **23**, one of the monomer precursors, and two diastereomeric epoxybenzo[*k*]fluoranthenes were elucidated by single-crystal X-ray crystallography.

Keywords: arenes · cyclooligomerization · Diels–Alder reaction · macrocycles · strain

Introduction

The synthesis of double-stranded polymers by poly-Diels–Alder (DA) addition[1] is occasionally accompanied by the formation of cyclic dimers and trimers.[2] If linear oligomers attain conformations, during the first growth steps, that allow a facile ring closure, cyclization can evidently compete with linear growth. In certain cases, conditions can be found under which cyclization becomes the main reaction. Double-stranded cycles have always been appealing synthesis targets, for example, to study orbital interactions and host–guest phenomena. Compounds with all-carbon skeletons, which are potential precursors of [*n*]cyclacenes (**1**) and [*n*]beltenes (**2**),

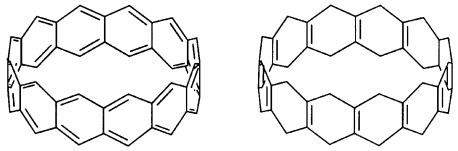

1 **2**

were of special interest for a couple of years.[2, 3] All attempts to generate [*n*]cyclacenes failed, presumably because of their predicted high reactivity.[4] According to density functional calculations, for example, they should have a triplet ground state.[5] In a sense, cyclacenes resemble the infinite, hypothetical polyacene.

Recently attempts to obtain less reactive, yet still double-stranded cycles were reported and the near future will show whether they can be converted into their respective unsaturated analogues.[6] Though not applied in all cases, the main synthetic tool is a electrocyclic ring-closure reaction, such as a Diels–Alder reaction. Attempts were made to develop rational syntheses for representatives, the most developed being the so-called "substrate-directed synthesis" by Stoddart and co-workers.[3a] This attempt is also based upon DA chemistry; it utilizes bifunctional components with appropri-

[a] Prof. Dr. A. D. Schlüter, Dr. W. D. Neudorff
Institut für Chemie, Organische Chemie,
Freie Universität Berlin
Takustrasse 3, 14195 Berlin (Germany)
Fax: (+49) 30-838-53357
E-mail: adschlue@chemie.fu-berlin.de

[b] Dr. D. Lentz, M. Anibarro
Institut für Chemie, Anorganische und Analytische Chemie
Freie Universität Berlin
Fabeckstrasse 34–36, 14195 Berlin (Germany)
Fax: (+49) 30-838-52424
E-mail: lentz@chemie.fu-berlin.de

Supporting information for this article is available on the WWW under http://www.wiley-vch.de/home/chemistry/ or from the author. It contains a) a suggestion for a nomenclature system for "fluoranthene-like" PAHs (SI Chart 1), b) AM1-calculated properties of [2.2.*q*]circocenes, [2.*q*:2.*q* − 1]circocenes, [2.2.*q*]fluoranthenes, [2.*q*:2.*q* − 1]fluoranthenes with $q = 1-5$ and $q - 1 > 0$, [*n*]cyclacenes with $n = 4-16$ (SI Tables 1–3); c) AM1-calculated gas-phase PAs of circocenes for different sites of protonation (SI Chart 2); d) List of structures (with ΔH_f values) used to calculate the MSE of $\mathbf{A}_r$ (SI Charts 3 and 4); e) Calculated MSEs and dehydration enthalpies for series $\mathbf{A}_r$, $\mathbf{C}_r$ and a second set $\mathbf{B}_r$, $\mathbf{D}_r$ (SI Figure 1, SI Tables 4 and 5); f) ^{1}H NMR spectra of **16** (SI Figure 2); g) ^{1}H NMR spectra of **17** (SI Figure 3); h) NMR spectra of the reaction **19** → **27** → **19** (SI Figure 4).

 DOI: 10.1002/chem.200304824

ate curvature and high *endo–exo* stereoselectivity, and also allows for a predictable cyclization to occur. None of the double-stranded cycles with an all-carbon frame available nowadays can be completely converted into their fully unsaturated analogues yet. Some time ago, we showed that a complete aromatization of DA polymers can be achieved when this process leads to macromolecules with fullerene-like structural elements, as in **3** and **4**.[7] The incorporation of *peri*-condensed naphthalene units with two adjacent five-membered rings considerably stabilizes the resulting polycyclic

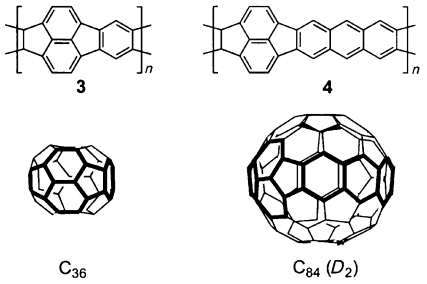

aromatic compounds (PAHs) compared with PAHs with a polyacene structure. This was a motivation for us to develop a synthetic strategy towards double-stranded cycles whose carbon skeletons resembles the belt-regions of fullerenes (here: C_{84} fullerene with D_2 symmetry) and can thus serve as potential precursors for the unsaturated analogues. Other strategies for fragments of fullerene structures have recently appeared.[8] Here we report on the synthesis of the carbon skeleton of the equator region of fullerene C_{84} by cyclodimerization of in-situ-generated isobenzofuran AB-type Diels–Alder (DA) monomers, X-ray characterization of the cyclization product, first steps toward aromatization, and the influence of strain energy on the outcome of the aromatization.

Results and Discussion

The polymerization of the in-situ-prepared AA-type DA monomer **5** with its BB-counterpart **6**, which leads to a substituted version of polymer **4**, is not accompanied by cyclization. Only linear structures are formed according to gel

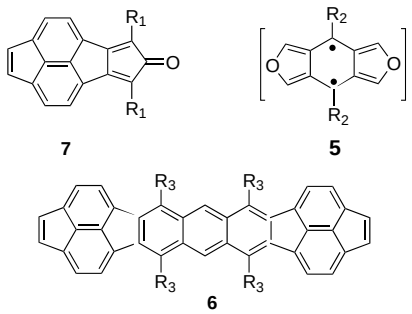

permeation chromatography (GPC) of the raw material.[7b] Evidently the distance between the respective two termini is not commensurable, and the attainment of a curved conformation of **6** is too costly in terms of energy for a cyclic 1:1 adduct to form. The stereoselectivity of the DA reaction between a acenaphthylene dienophile and an isobenzofuran-type diene is low. The formation of a cyclic 2:2 adduct is, therefore, unlikely to occur under step-growth conditions. AB-type monomer **7**, which proved very successful in polymerizations to give derivatives of polymer **3**,[7a,c] did not seem to be a good candidate either. In contrast to other cyclopentadienones, such as tetracyclone and phencyclone,[9] carbonyl-containing adducts of cyclopentene-fused cyclopentadienones are stable only under special conditions.[10] Thus, it is reasonable to assume that, upon self-condensation of two molecules of **7**, carbon monoxide is eliminated faster than the second condensation step and that cyclization can take place. After carbon monoxide elimination, the attainment of a curved conformation again is too costly to form a cyclic dimer. Cycles with more than two units of **7** are unlikely to form for probability reasons.

We therefore developed the route to building block **18** (Scheme 3), which should give cycle **19** upon dimerization. This route combines the following features:

1) According to model studies, dimers of **18** with the correct stereochemistry should react to give an unstrained 1:1 cycle.
2) The shape of the open-chain dimer, unlike **7**, remains unchanged until cyclization occurs.
3) The ether bridges in the oxanorbornene units of the cycle **19** can potentially be removed under aromatization, namely, by dehydration.

Dihydropyracylene **12** (Scheme 1) was selected as the source of the naphthalene unit and the adjacent five-membered rings of the target cycle **19**. Compound **12** is

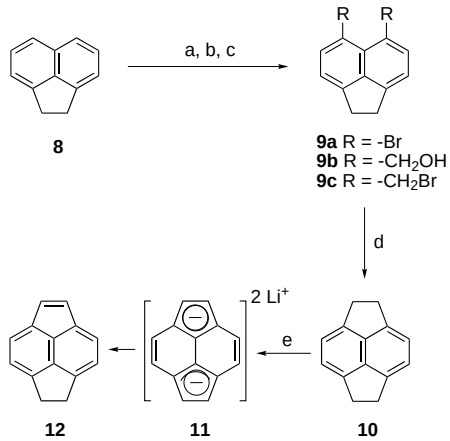

Scheme 1. Synthesis of dihydropyracylene **12**. a) NBS/DMF; b) BuLi, paraformaldehyde; c) PBr_3; d) PhLi; e) BuLi/TMEDA, $[Cu^{II}(acac)_2]$.

known;[11] however, it has not been used in synthetic chemistry, presumably because of its limited accessibility. Only its deprotonation has been studied so far.[12] To make larger quantities of this hydrocarbon available, a route was devised which is similar to the one developed by Trost et al.[11c]

However, diol **9b** was prepared through the intermediate dibromide **9a**, which is readily available from direct bromination of acenaphthene **8**;[13] this saves two steps. The final dehydrogenation reaction from **10** to **12** with dichlorodicyano *p*-benzoquinone (DDQ) was reported to proceed with 42% yield. Despite numerous attempts, we were unable to reproducibly achieve yields higher than 10–15%. Therefore, we decided to synthesize compound **12** via **11** by a dilithiation/oxidation sequence.[14] Dianion **11** was obtained by deprotonation with a slight excess of butyl lithium in the presence of tetramethylethylene diamine (TMEDA) and oxidized with Cu(II) acetylacetonate [$Cu(acac)_2$]. These reactions are easy to perform and gave compound **12** in 70–75% yield on the 10 g scale. Evidence for the stabilization of dianion **11** as a cyclopentadienyl–allyl system is provided by a dinuclear iron carbonyl complex of acenaphthylene.[15] These modifications rendered this important hydrocarbon a synthetically accessible compound and its chemistry can now be explored.

The synthesis of the AB-type DA-monomer precursors **17** is shown in Scheme 2. Under standard conditions, compound **12** and the isobenzofuran precursor **13**[16] gave the *endo* and *exo* isomers of **14** in a ratio of 4:1 (^{1}H NMR) and a total yield >90%. They were separated on the 10 g scale by column chromatography and obtained as analytically pure compounds. Subsequent dehydrogenation to **15** was carried out with DDQ and proceeded reproducibly with yields of 70–80%. Both diastereomers of **15** were now independently subjected to furan addition[17] to furnish the four diastereomeric oxanorbornenes **16** in the following ratios: *endo-syn:endo-anti* = 1.5:1 and *exo-syn:exo-anti* = 1:1 (^{1}H NMR). The yields of the final tetraphenylcyclopentadienone (tetracyclone) additions to the oxanorbornenes **16** to give **17** were not quite as high as expected because of a side reaction involving the attack of tetracyclone at the acenaphthylene termini as well in up to 20% yield. The resulting byproduct (not shown) was isolated and characterized for *endo-syn*-**17**. Nevertheless, the *endo*-isomers of **17** were isolated on the scale of a few grams and the *exo*-isomers on 0.5 g scale. All stereoisomers of compounds **14**–**17** were isolated by column chromatography and fully characterized on the basis of ^{1}H and ^{13}C NMR spectroscopy, elemental analysis, and/or high-resolution mass spectrometry.[18] The stereochemical assignment of isomers **14** rests upon common Karplus considerations of the dihedral HCCH angles at the ether bridge. This was further confirmed by the structures of the **22** isomers in the crystal (Figure 4). The assignment of the stereoisomers of **16** is based upon NOE measurements for the *endo* pair and on coupling pattern of the α-CH_2 groups for the *exo* pair. In analogy to related anthracene epoxides (not shown),[19] this group appears as a triplet for *exo-syn*-**16** and as AB-part of an ABCD spin system for *exo-anti*-**16**. The coupling patterns are further complicated because of reduced symmetry by the attached pyracene units of **16**; however, the initial coupling pattern remains visible. The stereochemistry of the isomers of **17** follows from the fact that all isomers of **16** were individually treated with tetracyclone. The addition of tetracyclone to the oxanorbornene termini proceeded stereospecifically in an *exo* fashion with *trans*-standing oxygen atoms in

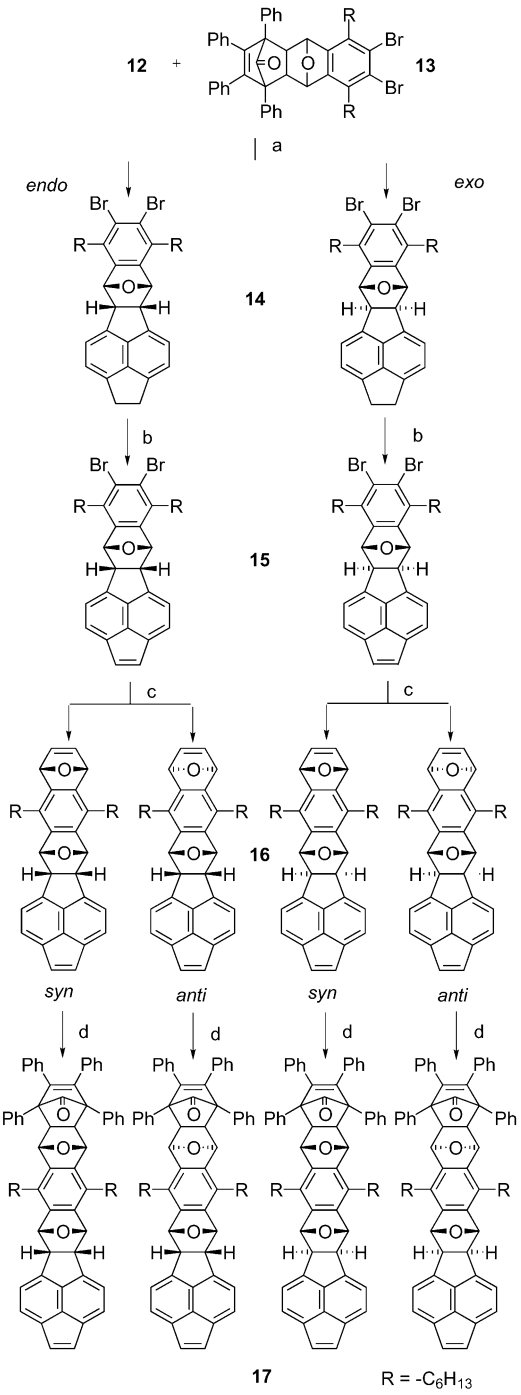

Scheme 2. Synthesis of the monomer precursors **17**. a) heat, toluene; b) DDQ, toluene; c) BuLi, furan; d) tetracyclone, EtOH.

general.[20] This was confirmed for *endo-syn*-**17** by single-crystal X-ray crystallographic analysis (Figure 1).

Cyclization reactions: Each of the four isomers of **17** were individually subjected to cyclization. The same macrocycle **19** was formed via the in-situ-generated AB-monomers *endo*-**18** and *exo*-**18** (Scheme 3). The cartoon-like representation in Figure 2 illustrates this important point. It shows the two different stereoisomers of **18** in the side view. Their olefinic termini are indicated by a double line and the isobenzofuran termini by an oxygen atom. Their configuration is indicated by both the kinks in the structure and the position of the oxygen

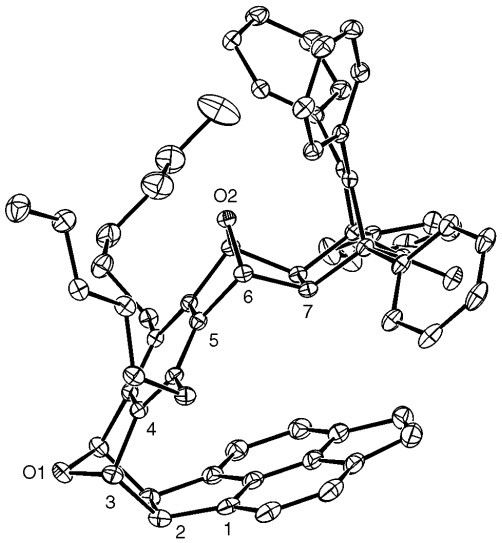

Figure 1. Structure of *endo-syn*-**17** in the crystal (ORTEP plot, 50% probability, H atoms not drawn). For the numbering scheme: see Table 1.

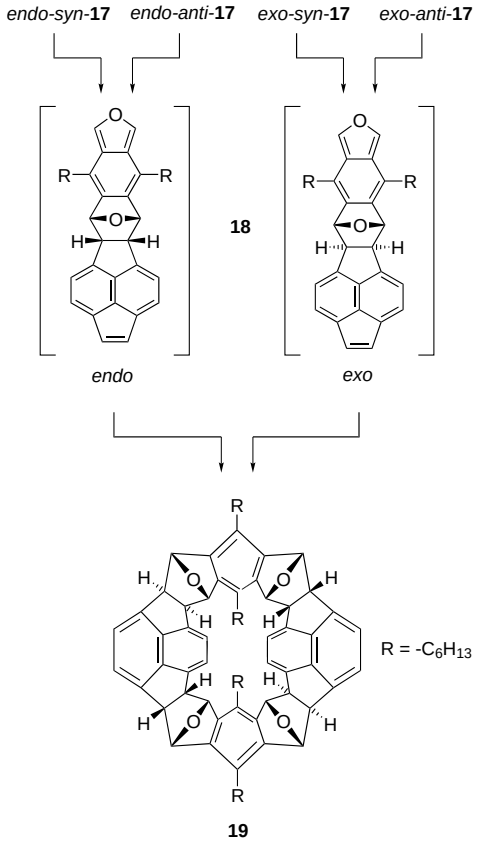

Scheme 3. Synthesis of the macrocycle **19** by cyclodimerization of the in-situ-generated AB-monomers **18**.

bridge. As can be seen, both the cyclization of two molecules of *endo*-**18** as well of two molecules of *exo*-**18** pass through different intermediates (both denoted as **18a**), but nevertheless give the same cycle **19**. This cartoon also makes clear how important it was to separate the isomers of **14** and individually convert them into their respective stereoisomers **17**. If steric constraints had been disregarded, the reaction of

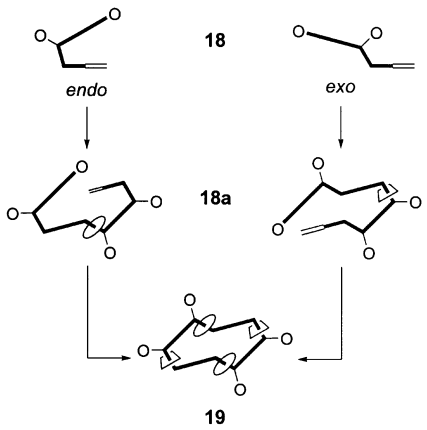

Figure 2. Schematic representation of the cyclodimerization of the isobenzofuran monomers **18** (side view) via the open chain dimers **18a**. Circles mark bonds formed during the reaction of *endo*-**18**, squares represent those of *exo*-**18**.

the four isomers of **17** and, thus, two isomers of **18** could have led to 32 diastereomeric open-chain dimers, such as **18a**. This would have resulted in grossly reduced cyclization yields, as all-mixed combinations of *endo*- and *exo*-**18** do not lead to cyclizible dimers. In contrast, individual reaction of the isomers of **18** reduces the number of statistically possible, diastereomeric open-chain dimers to eight for each of the two monomers; this statistically increases the cyclization probability by the factor of two. Of the 32 isomers, two can cyclize, compared to only one of the eight isomers. Up to 25% yield of **19** was obtained from the *endo* pair of **17** and up to 45% from the *exo* pair. These yields are higher than expected from simple statistical considerations, because, according to molecular models, not all of the eight isomers can actually be formed, especially for the *endo* case. For the *exo* case the higher yield can be attributed to the *endo* selectivity of the DA reaction.

Cycle **19** was purified both by size exclusion chromatography (SEC) or column chromatography. Its ^{1}H NMR spectrum showed a set of six signals for the six sets of heterotopic hydrogen atoms of its macrocyclic unit. Depending on its configuration, the methine protons of the oxanorbornene group show one set of two split signals (*endo*) and one set of two singlets (*exo*). The upfield shift to $\delta = 1.5$ ppm for one of the latter is in agreement with their position inside the cavity, facing the opposite naphthalene unit. The C_{2h} symmetry of the macrocyclic unit of **19** is also reflected in the broadband-decoupled ^{13}C NMR spectra, in which nine signals for the aromatic subunits and one set of two signals were found for the *endo* and the *exo* linkages, respectively. EI-MS revealed a strong molecular ion peak at $m/z = 1004$ corresponding to $[M]^+$. Additional confirmation of the structure of **19** was provided by an X-ray structural analysis (Figure 3) of single crystals grown from the diffusion of ethanol into a solution of **19** in chloroform. All four oxygen bridges of **19** are on the outer rim of the molecule. The carbon atoms of the *endo*-oxanorbornene groups are 11.6 Å apart from each other; the tertiary C atoms of the *exo*-oxanorbonene groups are 3.6 Å apart. Thus, the cavity is too small to incorporate other molecules.

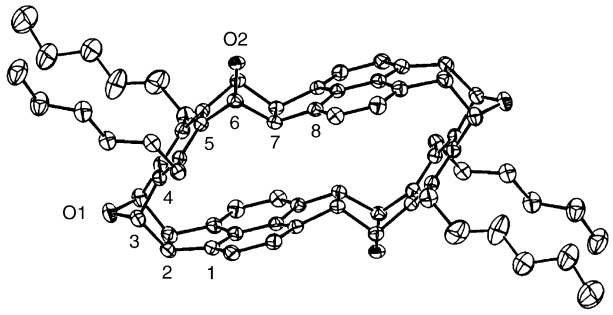

Figure 3. Structure of **19** in the crystal (ORTEP plot, 40% probability, H atoms not drawn). For the numbering scheme: see Table 1.

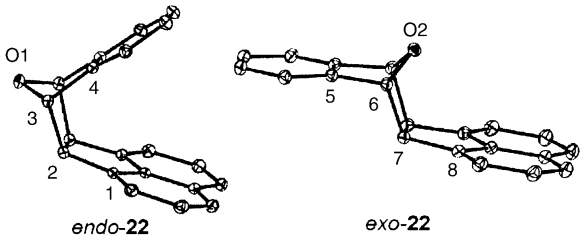

Figure 4. Structures of **22** in the crystal (ORTEP plot, 50% probability; H atoms not drawn). *endo*-**22** crystallizes with two molecules in the asymmetric unit (only one is shown). For the numbering scheme: see Table 1.

In addition to the above-mentioned higher-than-statistical yields for **19**, another remarkable result is that the cyclization can be carried out in bulk, in which normally linear polymerization is preferred. When 25 mg samples of neat monomer precursors **17** were heated to 200 °C for 1 h under high-vacuum conditions (0.02 mbar), cycle **19** was obtained in some cases. While cyclization could not be detected for *endo-syn*-**17**, *endo-anti*-**17** gave **19** in 10% yield and *exo-syn*-**17** gave cycle **19** in a yield of 40%. These yields are close to those obtained in the solution experiments.[18] The yields were determined by integration of the ^{1}H NMR spectra of the raw products and by SEC. The different behaviors of the *endo*-**17** pair can be explained by the steric demand of the [2.2.1]bicyclohepten-7-one group of *endo-syn*-**17**. This group blocks the approach of an *endo*-**18** molecule and forms a dimer that can cyclize. From the modeled structure of *endo-anti*-**17** (not shown) it becomes apparent that the [2.2.1]bicyclohepten-7-one group hinders such an approach far less. To our knowledge, these are the first examples of "bulk macrocyclizations" for double-stranded DA monomers.

As mentioned, one reason for the success of the above synthetic strategy was the unstrained nature of **19**. To confirm this, epoxybenzo[*k*]fluoranthene **22** (Scheme 4) was prepared from acenaphthene **20** and the isobenzofuran precursor **21**.[20] The *endo* and *exo* isomers of **22** were separated and individually characterized by X-ray structural analysis (Figure 4).

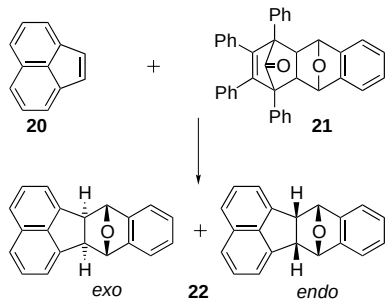

Scheme 4. Synthesis of diastereomeric epoxybenzo[*k*]fluoranthenes (**22**).

Table 1 gives selected bond lengths and angles for *endo-syn*-**17**, **19**, and **22**. Significant deviations of the structural parameters of **19** from those for the noncyclic structures are only found at the *exo*-oxanorbornene linkages. The C6-C7-C8 bond angle is increased by about 6° and the C5-C6-C7 bond angle is decreased by 3–4°. This is accompanied by a slight curvature of the aromatic units. These small structural differences confirm that the structurally closely related cycle **19** should actually be basically strainless.

Table 1. Selected bond lengths [Å] and angles [°] for *endo-syn*-**17**, **19**, **22**.

	19	*endo-syn*-**17**	*endo*-**22a**[a]	*endo*-**22b**[a]	*exo*-**22**
C1–C2[b]	1.518(2)	1.517(2)	1.518(1)	1.515(1)	
C2–C3	1.560(3)	1.566(2)	1.559(1)	1.562(1)	
C3–C4	1.509(3)	1.513(2)	1.512(1)	1.513(1)	
C5–C6	1.515(2)	1.520(2)			1.513(2)
C6–C7	1.547(2)	1.550(2)			1.561(2)
C7–C8	1.515(2)				1.515(2)
C1-C2-C3	116.62(17)	116.42(13)	117.59(7)	116.62(7)	
C2-C3-C4	107.68(14)	106.62(13)	108.29(6)	108.24(7)	
C5-C6-C7	103.88(14)	106.55(12)			107.83(9)
C6-C7-C8	118.92(15)				112.54(9)
C2-C3-O1	100.69(16)	101.30(12)	101.07(7)	100.86(7)	
O1-C3-C4	102.19(14)	102.40(12)	101.31(6)	101.43(7)	
C5-C6-O2	103.01(13)	101.56(11)			101.26(9)
O2-C6-C7	102.19(14)	101.83(11)			101.17(8)

[a] Two molecules in the asymmetric unit. [b] Atom numbering scheme according to Figures 1, 3, and 4. This numbering scheme was chosen for readability reasons and differs from the crystallographic numbering scheme.

Aromatization experiments: A number of predominately acid-catalyzed dehydration methods have been reported for the aromatization of oxygen-bridged compounds. None of them proved to be generally applicable. The method that employed *p*-toluene sulfonic acid monohydrate in a toluene solution has shown its efficiency with low-molecular-weight compounds and polymers structurally related to **19**.[7b, 21] Application of this method to **19** led to its complete consumption and furnished two products, the partly aromatized macrocycle **23** (Scheme 5) and an insoluble dark solid. Compound **23** was isolated by column chromatography in a yield of 49%, which is rather low relative to open-chain structures. The insoluble product has not been characterized further yet.

The ^{1}H NMR spectrum of **23** is similar to that of **19** except for the lack of singlets for the *exo*-configured oxanorbornene groups and an additional singlet of the *peri*-protons of the *ortho*-annulated naphthalene unit. Consequently, the ^{13}C NMR spectrum shows eleven signals for the aromatic carbon atoms along with only one set of two signals for the oxanorbornene linkages assigned to the *endo* configuration. EI-MS revealed the required molecular ion peak at $m/z = 968$.

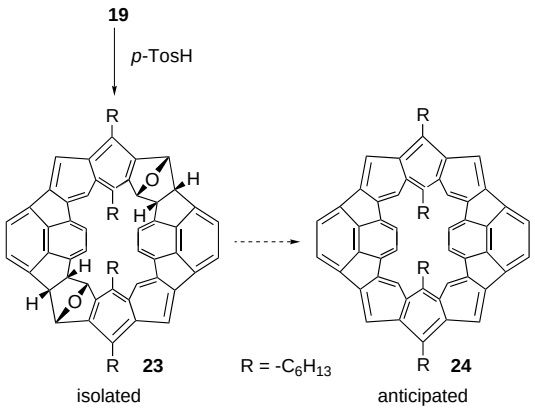

Scheme 5. Dehydration of **19**.

Final confirmation of the structure of **23** was provided by X-ray structural analysis (Figure 5) of a single crystal grown from diffusion hexane to a solution of **23** in chloroform. It

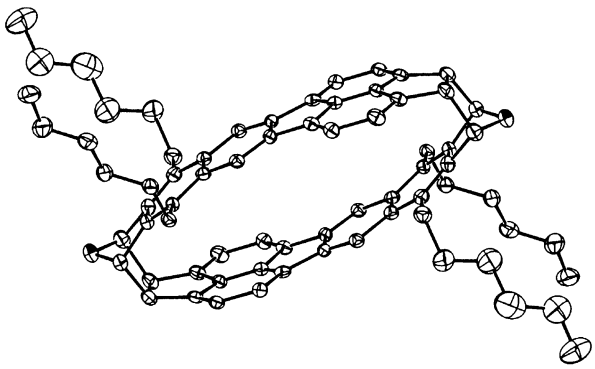

Figure 5. Structure of **23** in the crystal (ORTEP plot, 50% probability; H atoms not drawn).

shows an ellipsoidally flattened molecule whose benzo[*k*]-fluoranthene moieties are slightly bent. The maximum distance of these moieties is 4.1 Å at the center of the molecule. The central carbon atoms of the benzo[*k*]fluoranthene unit lie 1.3 Å over the plane that is defined by its four nearest saturated carbon atoms of the oxanorbornene linkages.

The seemingly selective aromatization of the *exo*-oxanorbornene groups is somewhat in contrast to earlier reports for open chain compounds in which the *endo*-configured groups react faster than the *exo* ones.[21] This was qualitatively confirmed by control experiments subjecting a 1:1 mixture of *endo*- and *exo*-**22** to the dehydration agent at room temperature. After 1 h, the *endo*:*exo* ratio had changed to 1:2.

The lack of any other dehydration product than **23**, including **24** from complete aromatization of **19**, was confirmed by NMR tube experiments in benzene that showed no other sharp signals than those for **19** and **23**. Applying harsher conditions to **23** by the use of a large excess of anhydrous *para*-toluene sulfonic acid (*p*-TosH) in refluxing toluene did not change the overall result, except for a higher reaction rate. It should be mentioned here, however, that the origin of the insoluble product is not yet clear and that it may be a follow-up product of a completely dehydrated material.

The results of the dehydration of **19** may be either attributed to a high reactivity of **24** towards its conversion into insoluble material, as is assumed for the [*n*]cyclacenes, or explained in terms of strain energy.[3d] The latter argument can be qualitatively derived from the X-ray structures of **19** and **23**. The dehydration of the *exo*-oxanorbornene groups causes fewer structural changes than would be the case for the dehydration of the *endo* groups. This is accompanied by a minor change in the strain energy of the product obtained by dehydration of the *exo* groups and may explain the unusual selectivity of the dehydration reaction. Further aromatization is associated with the transfer from the ellipsoidal shape of **23** to the round shape of **24** during which the major part of the strain energy has to be introduced. We call this type of strain energy MSE (macrocyclic strain energy), which originates from the macrocyclic structure, to distinguish it from the local strain, induced by the bicyclic oxanorbornene groups and five-membered rings, that is also present in the noncyclic compounds **14**–**18**. The consequence of the necessary introduction of MSE during dehydration of the *endo*-oxanorbornene groups becomes more clear by the first step of the acid-catalyzed dehydration mechanism. Though not well investigated, it is reasonable to assume that the oxygen bridge is opened after protonation (Scheme 6) to form the carbenium

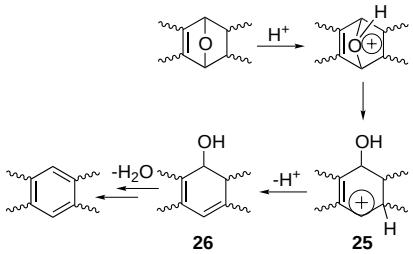

Scheme 6. Probable mechanism of acid-catalyzed dehydration of oxanorbornenes.

ion **25**, which in turn gives the cyclohexadienol structure **26** through the loss of a proton. Transferred to **23**, the major part of the MSE has to be raised in the step corresponding to the transition of **25** to **26**. Therefore, the planarization of two atoms has to take place against the pyramidalization of any of the sp^2-hybridized carbon atoms of the macrocyclic backbone at a time when the exothermic elimination of water cannot contribute. It is unlikely that a cyclohexadienol structure, such as **26**, is involved during the acid-catalyzed dehydration of the *endo*-oxanorbornene linkages of **19** or **23**, and rather destructive side reactions may take place instead.

On account of this consideration, further attempts with different methods of acid-catalyzed dehydration have not yet been undertaken. The use of iodotrimethylsilane (TMSI)[22] as the dehydration agent did not yield **24** or any other dehydration product. NMR spectroscopic monitoring showed a very clean reaction course (see the Supporting Information). Although we were unable to isolate the reaction product or obtain mass spectrometric evidence, structure **27** was tenta-

tively assigned on the basis of the following argumentation (Scheme 7).

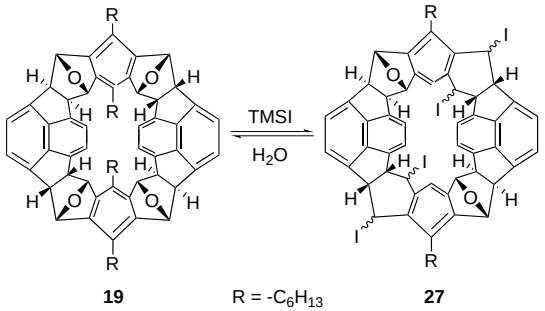

Scheme 7. Reaction of **27** with TMSI (inner R groups for **27** are not drawn).

The signals of the protons in the *endo*-oxanorbornene group are shifted downfield from $\delta = 5.73$ and 4.70 ppm for **19** to $\delta = 6.22$ and 4.83 ppm for **27**, respectively. These changes are accompanied by the loss of coupling. For the protons of the *exo* group, only the signal at $\delta = 5.13$ ppm for **19** is slightly shifted downfield to $\delta = 5.22$ ppm for **27**, whereas the other is shifted upfield from $\delta = 1.50$ ppm for **19** to $\delta = 1.10$ ppm for **27**; both remained as singlets. The ^{13}C NMR spectrum of **27** shows only one signal for carbons connected to oxygen at $\delta =$ 82.71 ppm, which is a typical shift for *exo*-oxanorbornene groups. A further and astounding piece of evidence for the formation of **27** is its almost complete backreaction to **19** in the presence of water.

We believe that the MSE, which has to be mainly built up in the final aromatization steps, is the dominant factor for the not yet surmounted problems with these very steps. As mentioned above, another reason may also be high reactivity of the completely aromatized **24** towards attack by electrophiles or polymerization. To obtain more insight into this matter, semiempirical AM1[23] calculations were performed. In this context a simple nomenclature was derived for structures such as **24** that is also applicable to various other belt-shaped PAHs (these compounds are called circocenes) as well as for oligomeric and polymeric open-chain PAHs (see the Supplementary Information).

Calculations: Semiempirical AM1[23] calculations on the unsubstituted parent compound and a series of eight homologues (**28** and **29**) were performed to estimate the reactivity of **24**. These compounds belong to two series, one with two equal *ortho*-annelated subunits called *simple* circocenes (**28**) and one with two different *ortho*-annelated subunits named *mixed* circocenes (**29**). These calculations were compared to earlier reported calculations on the same level of theory for linear acenes by Notario,[24] which showed good correlation with available experimental data, namely, ionization potentials. In addition, recently reported calculations for [*n*]cyclacenes ($n = 4-9$)[25] were reevaluated and extended to $n = 10-16$. Reevaluation was necessary because the reported values for the [5]cyclacene do not belong to a cyclacene structure, but rather to a Dewar benzene-type derivative and, therefore, showed, like the values for [6]cyclacene, a poor correlation to the values of the other compounds in this series.

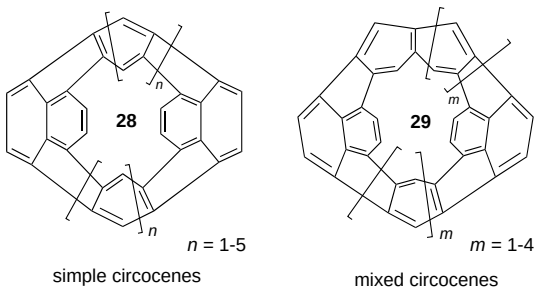

As a result, the values for the circocenes in comparison with those of linear acenes and [*n*]cyclacenes did not give an indication for an exceptionally high reactivity of the circocenes in general and **28** ($n = 3$) in particular. The HOMO–LUMO gaps for circocenes, linear acenes, and cyclacenes are given in Figure 6.

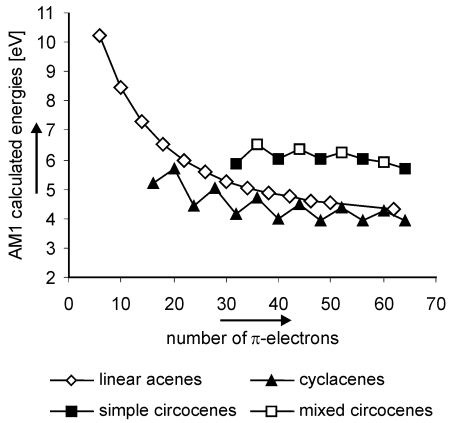

Figure 6. AM1 calculated HOMO–LUMO gaps of linear [*n*]acenes ($n = 1-12, 15$),[24] [*n*]cyclacenes ($n = 4-16$), simple circocenes ($n = 1-5$), mixed circocenes ($m = 1-4$).

The HOMO–LUMO gap can be correlated to the Diels–Alder reactivity of PAHs.[24] The HOMO–LUMO gaps for all circocenes are in the range of those of tetracene and hexacene. The gap for **28** ($n = 3$) is similar to that of pentacene. The increase of the HOMO–LUMO gaps for the simple circocenes up to **28** ($n = 3$) is similar to earlier reported calculations for polyfluoranthenes by Kertesz,[26] and is predominately a consequence of increasing LUMO energies.[27] In addition to these electronic properties, the gas-phase proton affinities (PA) for the circocenes were calculated for several protonation sites (see the Supplementary Information) according to Equation (1) and with the experimental value $\Delta H_f(H^+) = 367.2$ kcal mol^{-1}.[24]

$$PA = \Delta H_f(B) + \Delta H_f(H^+) - \Delta H_f(BH^+) \quad (1)$$

The PA of **28** ($n = 3$) was found to be 220.4 kcal mol^{-1} for protonation at the 9-position of the anthracene unit. This value lies between the calculated values for tetracene (215.9 kcal mol^{-1}) and pentacene (223.5 kcal mol^{-1}).[24] For comparison, the PAs of [*n*]cyclacenes with odd *n* were calculated to be in the range of 252–257 kcal mol^{-1}.[28]

Actually, a high reactivity of the circocenes cannot be ruled out for the failure of complete aromatization of **19** by this simple comparison on this level of theory, but it should be far less important than for the [*n*]cyclacenes.

The MSE, which has to be built up during aromatization to **24** does indeed seem to play a significant role in this context. The MSE was calculated for the unsubstituted parent compounds $\mathbf{A}_r$ (Figure 7) according to Equation (2).

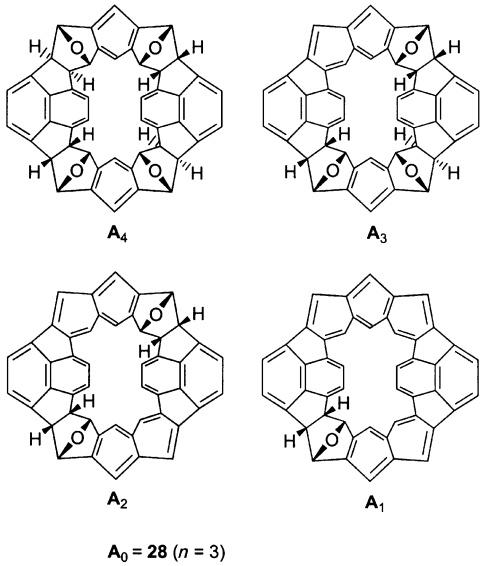

Figure 7. Structures of model compounds $\mathbf{A}_r$ (r = number of ether bridges) to calculate the development of the MSE during dehydration of **19**.

$$\mathrm{MSE} = \Delta H_f(\mathbf{A}_r) - \Delta H_f(\mathbf{C}_r) - \Delta H_{r(\mathrm{split})} - \Delta E_{\mathrm{res}} \quad (2)$$

In Equation (2) r denotes the number of ether bridges and $\mathbf{C}_r$ are open-chain model compounds derived from $\mathbf{A}_r$ by a hypothetical reductive cleavage of the macrocyclic molecules at an *endo* linkage (Scheme 8). These model compounds are

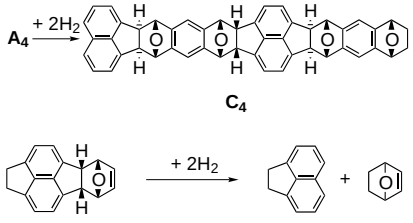

Scheme 8. Hypothetical reaction to derive noncyclic model compounds $\mathbf{C}_r$ of $\mathbf{A}_r$ (above). Sample of a model reaction to calculate $\Delta H_{r(\mathrm{split})}$ (below).

considered to be free of MSE, which was examined on a second set of model compounds (see the Supporting Information). $\Delta H_{r(\mathrm{split})}$ is the enthalpy of the cleavage reaction. The value for $\Delta H_{r(\mathrm{split})}$ was calculated as the average from a series of five model reactions (one example is given in Scheme 8) to be 34.2 ± 1.2 kcal mol^{-1} (for $\Delta H_f(\mathrm{H}_{2(\mathrm{gas})}) = 0$ kcal mol^{-1}). ΔE_{res} is the change in resonance energy on extending the π system in every dehydration step. Except for $\mathbf{A}_0$, this value equals zero because $\mathbf{A}_{1-4}$ and $\mathbf{C}_{1-4}$ have the same π system, and that part of ΔE_{res} which results from a bending of the π system is considered to be a part of the MSE. The change in resonance energy for $\mathbf{A}_1 \rightarrow \mathbf{A}_0$ was not calculated explicitly. Therefore, the MSE of $\mathbf{A}_0$ differs by this amount.

The calculated MSEs for $\mathbf{A}_r$ are given in Table 2. The MSE of $\mathbf{A}_4$ is 12 kcal mol^{-1} and thus very low. This is in good agreement with the result from the crystallographic analysis.

Table 2. AM1-calculated macrocyclic strain energies (MSE).

	$\mathbf{A}_4$	$\mathbf{A}_3$	$\mathbf{A}_2$	$\mathbf{A}_1$	$\mathbf{A}_0$
MSE	12.0	16.0	16.5	85.7	122.5

The MSE of $\mathbf{A}_0$ is 122.5 kcal mol^{-1}; this indicates that every five- and six-membered ring has to carry ≈9 kcal mol^{-1} of the MSE. This is not an exceptionally high value compared to other compounds.[29] The critical point is the change in MSE on going from $\mathbf{A}_2 \rightarrow \mathbf{A}_1$. In this step, the first *endo*-oxanorbornene group is aromatized. Approximately 57 % of the total MSE of $\mathbf{A}_0$ has to be built up during this step. This is also reflected by the heats of reaction (Table 3) calculated with the use of the experimental $\Delta H_f(\mathrm{H_2O_{(gas)}}) = 57.8$ kcal mol^{-1}.[30]

Table 3. AM1-calculated heats of reaction.

Reaction	ΔH_r [kcal mol^{-1}]
$\mathbf{A}_4 \rightarrow \mathbf{A}_3 + \mathrm{H_2O}$	−24.6
$\mathbf{A}_3 \rightarrow \mathbf{A}_2 + \mathrm{H_2O}$	−26.6
$\mathbf{A}_2 \rightarrow \mathbf{A}_1 + \mathrm{H_2O}$	+44.6
$\mathbf{A}_1 \rightarrow \mathbf{A}_0 + \mathrm{H_2O}$	+14.9
$\mathbf{A}_4 \rightarrow \mathbf{A}_0 + 4\ \mathrm{H_2O}$	+8.3

The first two dehydration steps of the *exo*-oxanorbornene groups are exothermic with ≈25 kcal mol^{-1}. This is a similar value to those values calculated for all steps of the dehydration of the open-chain model compounds $\mathbf{C}_r$ (see the Supporting Information). On the other hand, the dehydration of the first *endo* group is the most endothermic step with 45 kcal mol^{-1}. The endothermic dehydration of both *endo* groups makes the overall aromatization slightly endothermic. These results can be correlated with the experimental observations:

1) The lack of NMR spectroscopic evidence of a single dehydration product of **19** and the formation of **23** is in good agreement with the calculated exothermicity of these dehydration reactions, accompanied by minor changes in the MSE.
2) The lack of an indication for a dehydration product of an *endo*-oxanorbornene group correlates with the calculated endothermy of these reaction steps, which is caused by a strong increase of the MSE.
3) The failure of HI elimination of **27** and its back reaction to **19** can also be explained by the necessary increase of the MSE.

Therefore, we consider the build-up of MSE to be an important factor with respect to the lack of complete aromatization of **19** under the applied conditions. Because all the precursors prepared so far for the all-carbon, double-

stranded, belt-shaped aromatics have to pass a flat intermediate structure similar to **23** during complete aromatization. The problem of building up MSE may be a general one for the synthesis of belt-shaped aromatics to succeed. The work by Cory also points in this direction.[3b]

Conclusion

The belt-shaped compound **19** is the first representative of a double-stranded macrocycle with a carbon skeleton similar to the equatorial region of a fullerene and thus is a potential precursor for the fully unsaturated analogue **24**. Macrocycle **19** was constructed from bifunctional, in-situ-generated Diels–Alder building blocks *endo*-**18** and *exo*-**18**; this afforded **19** in yields of up to 45%. Insights into stereochemical details of the sequence and its implications regarding the course of cyclization are discussed. In order to make these building blocks conveniently available, the synthesis of the known dihydropyracylene (**12**), which is a sequence key compound, was optimized so that it is now available on the 10 g scale in a few simple steps. This improvement not only had considerable impact on the sequence described here, but also makes **12** a valuable starting material for the future synthesis of fullerene parts and related compounds, a presently heavily pursued research area. Attempts to completely aromatize **19** yielded a partly aromatized macrocycle **23**, which, like **19**, was characterized by single-crystal X-ray diffraction. It also furnished an insoluble material, which will be investigated further. Semiempirical AM1 calculations indicate the required build-up of strain energy during the conversion of **23** to the fully unsaturated belt **24** as a main reason for the incomplete aromatization. In this context a simple to use so-called [*f.p.q*] nomenclature for a wide variety of open-chain and cyclic PAHs was suggested.

Experimental Section

X-ray crystal structures: Crystals of suitable for X-ray diffraction measurements were grown from ethanol (*endo-syn*-**17**, *endo*-**22**, *exo*-**22**) and by diffusion of ethanol or hexane into a solution of the compound in chloroform (**19** and **23**, respectively). Crystals of **23** contained solvent molecules and therefore tend to disintegrate with loss of the solvent outside saturated solutions, therefore the crystal was mounted at low temperature on the tip of a glass fiber. The data of **19** were collected on a Enraf Nonius Turbo CAD4 at ambient temperature with $Cu_{K\alpha}$ irradiation. The data collection of *endo-syn*-**17**, *endo*-**22**, *exo*-**22**, and **23** was performed at low temperature with a BRUKER-AXS SMART CCD diffractometer ($Mo_{K\alpha}$). A total of 600 frames ($\Delta\omega = 0.3^\circ$) for each run were collected for three ϕ positions (0°, 90°, and 240°) resulting in 1800 frames for each data set. The data were reduced to F_o^2 and corrected for absorption effects by using SAINT[31] and SADABS,[32] respectively. The structures were solved with direct methods and refined with full-matrix least-squares on F^2 (SHELXL 97[33]). The quality of the structure determination of **23** was strongly influenced by the fact that the crystal contained disordered chloroform solvate molecules and that one side chain also showed some disorder. The electron density of the solvate molecules was taken into account by means of the squeeze option of the program package PLATON.[34] Details on the data collection and structure refinement are listed in Table 4. ORTEP[35] for Windows was used for to prepare the graphical representations. WINGX[36] was used for the crystallographic computing.

Table 4. Crystal data and structure refinement for **19**, *endo-syn*-**17**, *endo*-**22**, *exo*-**22**, and **23**.

Compound	**19**	*endo-syn*-**17**	*endo*-**22**	*exo*-**22**	**23**
formula	$C_{72}H_{76}O_4$	$C_{67}H_{60}O_3$	$C_{20}H_{14}O$	$C_{20}H_{14}O$	$C_{72}H_{72}O_2$
M_r	1005.32	913.15	270.13	270.13	969.30
T [K]	293(2)	153(2)	133(2)	133(2)	163(2)
λ [Å]	1.54060	0.71073	0.71073	0.71073	0.71073
crystal system	orthorhombic	monoclinic	triclinic	orthorhombic	monoclinic
space group	*Pbca*	$P2_1/c$	$P\bar{1}$	$Pna2_1$	$P2_1/c$
a [Å]	10.176(5)	20.059(2)	9.1071(6)	11.7977(9)	14.8104(6)
b [Å]	16.040(5)	15.356(3)	12.3014(9)	21.8171(16)	13.7155(5)
c [Å]	33.421(5)	17.470(3)	12.9394(9)	5.2400(4)	14.4770(5)
α [°]	90	90	73.1020(10)	90	90
β [°]	90	112.745(12)	76.9600(10)	90	95.2100(10)
γ [°]	90	90	87.076(2)	90	90
V [Å^3]	5455(3)	4962.6(12)	1351.08(16)	1348.73(18)	2928.59(19)
Z	4	4	4	4	2
ρ_{calcd} [mg m^{-3}]	1.224	1.222	1.329	1.331	1.099
μ [mm^{-1}]	0.567	0.073	0.080	0.080	0.064
$F(000)$	2160	1944	568	568	1040
crystal size [mm^3]	0.8 × 0.7 × 0.3	1.0 × 0.82 × 0.07	1.0 × 0.6 × 0.32	1.6 × 0.32 × 0.2	0.3 × 0.24 × 0.08
θ range [°]	2.64–59.91	1.83–26.36	1.69–33.17	1.87–33.10	1.38–23.25
index ranges	$-11 \le h \le 11$ $-18 \le k \le 0$ $-37 \le l \le 0$	$-25 \le h \le 23$ $-19 \le k \le 19$ $-21 \le l \le 21$	$-13 \le h \le 13$ $-18 \le k \le 18$ $-19 \le l \le 19$	$-17 \le h \le 17$ $-33 \le k \le 32$ $-7 \le l \le 7$	$-16 \le h \le 16$ $-15 \le k \le 15$ $-16 \le l \le 16$
reflections collected	7653	45808	36325	17520	22082
independent reflections [R(int)]	4039 [0.0856]	10134 [0.0296]	9714 [0.0282]	4788 [0.0538]	4209 [0.060]
completeness to θ	59.91°, 99.9%	26.36°, 99.9%	33.17°, 94.4%	33.10°, 95.8%	23.25°, 100%
data/restraints/parameters	4039/460/374	10134/0/633	9714/0/379	4788/1/190	4209/0/336
quality-of-fit on F^2	1.067	1.013	1.006	1.075	1.541
final R indices [$I > 2\sigma(I)$] R_1/wR_2	0.0486/0.1261	0.0434/0.1150	0.0446/0.1307	0.0493/0.1215	0.1209/0.3627
R indices (all data) R_1/wR_2	0.0526/0.1298	0.0605/0.1292	0.0522/0.1379	0.0521/0.1251	0.1479/0.3861
largest diff. peak/hole [e Å^{-3}]	0.194/−0.193	0.444/−0.357	0.459/−0.261	0.366/−0.244	2.369/−0.616

CCDC-202685 (*endo-syn*-**17**), CCDC-202682 (**19**), CCDC-202681 (*exo*-**22**), CCDC-202684 (*endo*-**22**), CCDC-202683 (**23**) contain the supplementary crystallographic data for this paper. These data can be obtained free of charge via www.ccdc.cam.ac.uk/conts/retrieving.html (or from the Cambridge Crystallographic Data Centre, 12 Union Road, Cambridge CB21EZ, UK; fax: (+44) 1223-336033; or deposit@ccdc.cam.uk).

Computation: All calculations were performed with the HyperChem 6.02 package.[37] The AM1 method at the restricted Hartree–Fock (RHF) level and conjugate gradient minimization, Polak–Ribiere approach, were applied to obtain the optimized geometries. The convergence limit and gradient values (RMS) were maintained below 10^{-4} kcal mol^{-1} and 0.01 kcal Å^{-1} for macrocyclic structures and below 10^{-4} kcal mol^{-1} and 0.1 kcal Å^{-1} for open-chain structures. Minimum structures for [5]cyclacene and [6]cyclacene could be obtained starting from preoptimization with the implemented mm+ force-field followed by AM1 optimization applying a convergence limit and an RMS of 10^{-5} kcal mol^{-1} and 10^{-6} kcal Å^{-1}, respectively. These minimum structures were checked by frequency analysis.

General preparative methods: All readily available reagents were used without further purification. Solvents were purified and dried by standard procedures. All reactions were carried out under nitrogen. NMR spectra were recorded in $CDCl_3$ (unless otherwise stated) either on Bruker WH 270 MHz or AC 500 MHz spectrometers, with the solvent as the internal standard. Mass spectra (MS) were obtained from Varian MAT 771 or MAT 112 S, respectively. The matrix used for fast atom bombardment (FAB) spectra was 3-nitrobenzyl alcohol (NOBA). Column chromatography was carried out on silica gel 60 (230–400 mesh, Merck). Thin-layer chromatography (TLC) was performed on aluminum sheets coated with Merck 5554 silica gel 60F, visualization by an ultraviolet (UV) lamp (λ = 254 nm and λ = 366 nm). Analytical size exclusion chromatography (SEC) was performed on Waters Assoc. 150-c Alc/GPC chromatograph on Waters Styragel HR columns and with tetrahydrofuran (THF) as the mobile phase. A Waters 484 UV/Vis detector was used with a polystyrene standard. Melting points were determined on a Büchi 500 and are uncorrected.

5,6-Dibromoacenaphthene (9a): This was prepared by a modified Kasai method:[13] a suspension of *N*-bromosuccinimide (NBS) (1 kg, 5.62 mol) in DMF (2 L) was added in portions to an ice-cooled suspension of acenaphthene (400 g, 2.59 mol) in DMF (500 mL) over a period of 5 h. The temperature of mixture was not allowed exceed 15 °C. The mixture was stirred for a further 12 h and then allowed to warm to room temperature. The precipitate was filtered with suction, washed with ethanol (3 × 500 mL), and purified by stirring over night in refluxing ethanol (3 L). Cooling to room temperature, filtration, washing with ethanol, and drying in vacuo yielded 206 g (25 %) of a beige crystalline solid (m.p. 169–172 °C) that was suitable for further work. Recrystallization of a sample in chloroform raised the melting point to 173–175 °C (lit.:[12] 174–176 °C). ^{1}H NMR: δ = 3.28 (s, 4H; H-1,2), 7.06 (d, ^3J = 7.49 Hz, 2H; H-3,8), 7.76 ppm (d, ^3J = 7.49 Hz, 2H; H-4,7); ^{13}C NMR (68 MHz, $CDCl_3$): δ = 29.99 (C-1,2), 114.31, 120.87, 131.80, 135.77, 141.75, 147 ppm (arom-C)

5,6-Bis(hydroxymethyl)acenaphthene (9b): A suspension of **9a** (40 g, 129 mmol) in dry diethyl ether was prepared under nitrogen and cooled to −30 °C. BuLi (1.6 M, 170 mL, 272 mmol) in hexane was added within 10 min. After further 30 min of stirring, paraformaldehyde (8 g, dried over P_2O_5) was added at once. The mixture was stirred for 3 h at −30 °C and for a further 16 h while warming to room temperature. The reaction was quenched by adding HCl (40 mL, 25 %). After 1 h of stirring, the colorless precipitate was filtered with suction, suspended in diethyl ether (500 mL), filtered again, and dried in vacuum at 50 °C. The dry material was powdered and suspended in 1 % HCl for 2 h, filtered, washed with ethanol (2 × 100 mL), and dried again in vacuum at 50 °C yielding 20.5 g (74 %) of a colorless solid (m.p. 201–203 °C), which was suitable for further work. Two recrystallizations from dioxane raised the melting point to 201–204 °C (lit.:[11c] 202–205 °C). ^{1}H NMR ([D$_6$]DMSO): δ = 2.15 (s, 4H; H-1,2), 3.85 (d, ^3J = 5.3 Hz, 4H; CH_2OH), 4.25 (t, ^3J = 5.3 Hz, 2H; OH), 6.09 (d, ^3J = 7.0 Hz, 2H; H-3,8 or H-4,7), 6.35 ppm (d, ^3J = 7.0 Hz, 2H; H-3,8 or H-4,7); ^{1}H NMR ([D$_6$]DMSO/D$_2$O): 1.96 (s, 4H; H-1,2), 3.67 (s, 4H; CH_2OH), 5.95 (d, ^3J = 7.0 Hz, 2H; H-3,8 or H-4,7), 6.34 ppm (d, ^3J = 7.0 Hz, 2H; H-3,8 or H-4,7); ^{13}C NMR ([D$_6$]DMSO): δ = 29.46 (C-1,2), 63.05 (CH_2OH), 118.96, 128.53, 129.70, 134.11, 140.24, 145.92 ppm (arom-C); MS (80 eV, EI, 100 °C): *m*/*z* (%): 214 (30) $[M]^+$, 196 (100) $[M-H_2O]^+$, 167 (69) $[M-H_2O-HCO]^+$.

Bis(bromomethyl)acenaphthene (9c): Compound **9c** was prepared from **9b** (20 g, 93 mmol) according to a published procedure[11c] in 83 % yield (26.2 g). M.p. 157–159 °C (decomp) (lit:[10c] 157–159 °C); ^{1}H NMR: δ = 3.33 (s, 4H; H-1,2), 5.28 (s, 4H; CH_2Br), 7.26 (d, ^3J = 7.23 Hz, 2H; H-3,8), 7.55 ppm (d, ^3J = 7.23 Hz, 2H; H-4,7); ^{13}C NMR: δ = 30.16 (C-1,2), 36.81 (CH_2Br), 119.96, 127.75, 129.44, 134.02, 140.92, 149.34 ppm (arom-C)

Pyracene (10): This was prepared by a modified Trost method:[11c] A solution of **9c** (28 g, 82 mmol) in dry diethyl ether (120 mL) was added to an ice-cooled mixture of PhLi (50 mL, 90 mmol, 1.8 M in cyclohexane/diethyl ether) over a period of 10 min. The mixture was stirred for 4 h and was then quenched with water (10 mL). The organic solvent was evaporated, the residue dissolved in CH_2Cl_2 (1 L), and the organic layer was washed with water. Drying and evaporation of the solvent yielded crude **10** which was further purified by digestion in warm diethyl ether. After cooling to room temperature the precipitate was filtered and dried in vacuum. This procedure was repeated once to yield 13.7 g (93 %) of a colorless solid (m.p. 205–209 °C), which was suitable for further work. Sublimation of a sample raised the melting point to 212–216 °C (lit.:[11c] 214–217 °C); ^{1}H NMR: δ = 3.42 (s, 8H; H-1,2,5,6), 7.19 ppm (s, 4H; H-2,3,7,8); ^{13}C NMR: δ = 31.60 (C-1,2,5,6), 120.33, 138.35, 140.81 ppm (arom-C); MS (80 eV, EI, 100 °C): *m*/*z* (%): 180 (100) $[M]^+$.

1,2-Dihydropyracylene (12): Under nitrogen atmosphere, a solution of **10** (13.7 g, 76 mmol) and TMEDA (30 mL) in dry cyclohexane (250 mL) was prepared. BuLi (110 mL of a 1.6 M solution in hexane) was added to this solution over a period of 10 min at room temperature. The color changed quickly to dark red and then to dark green. After refluxing for 1 h, the mixture was allowed to cool for 15 min and then added dropwise to an ice-cooled suspension of [Cu(II)(acac)$_2$] (50 g, 190 mmol) in dry cyclohexane (150 mL) over a period of 15 min. The mixture was stirred for another 30 min and then poured onto a short column (Al_2O_3, basic, activity grade V, height of column 5 cm) and washed with hexane until the filtrate became colorless. The solvent was evaporated in a vacuum, and the crude yellow-brown product was purified by column chromatography (silica gel, hexane/ethyl acetate 10:1, R_f = 0.57) to yield 10.01 g (74 %) of a yellow crystalline solid (m.p. 154–156 °C) (lit:[11c] 156–157 °C); ^{1}H NMR: δ = 3.50 (s, 4H; H-1,2), 7.16 (s, 2H; H-5,6), 7.41 (d, ^3J = 6.9 Hz, 2H; H-3,8), 7.77 ppm (d, ^3J = 6.9 Hz, 2H; H-4,7); ^{13}C NMR: δ = 32.37 (C-1,2), 120.46 (C-3,8), 126.01 (C-3,4,7,8), 127.93 (C-8c), 128.22 (C-5,6), 134.90 (C-8b), 135.22 (C-4a,6a), 146.60 ppm (C-2a,8a).

1,2,4b,5,10,10a-Hexahydro-7,8-dibromo-5,10-epoxy-6,9-dihexylbenzo[*k*]cyclopenta[*c*,*d*]fluoranthene (14): A solution of **12** (3.56 g, 19.8 mmol) and **13**[16] (16.9 g, 19.8 mmol) in toluene (300 mL) was prepared and refluxed for 24 h. After cooling to room temperature, the solvent was evaporated in vacuo. To remove a large part of the tetraphenylbenzene byproduct (≈80 %), the residue was suspended in a 2:1 mixture of hexane/toluene (50 mL) and stirred for 30 min. The suspension was filtered with suction, and the residue washed with a 2:1 mixture of hexane/toluene (2 × 25 mL). The combined organic layers were concentrated to dryness in vacuo. The isomers were purified and separated by column chromatography (silica gel, hexane/toluene 2:1) to give 2.12 g of *exo*-**14** (m.p. 126–127 °C, R_f = 0.20) and 8.61 g of *endo*-**14** (m.p. 92–94 °C, R_f = 0.14) in a combined yield of 97 %.

exo-***14***: ^{1}H NMR: δ = 0.96 (t, 6H, ^3J = 7.1 Hz; CH_3), 1.3–1.6 (m, 12H; alkyl-CH_2), 1.73 (m, 4H; β-CH_2), 2.95 (m, 4H; α-CH_2), 3.43 (s, 4H; H-1,2), 3.92 (s, 2H; H-4b,10a), 5.41 (s, 2H; H-5,10), 7.28 (d, ^3J = 6.9 Hz, 2H; H-3,12), 7.37 ppm (d, ^3J = 6.9 Hz, 2H; H-4,11); ^{13}C NMR (125 MHz): δ = 14.12, 22.61, 29.46, 31.56, 31.69, 35.09 (alkyl-C and C-1,2), 55.14 (C-4b,10a), 83.44 (C-5,10), 120.67, 126.16, 134.34, 138.13, 140.41, 142.49, 144.56 ppm (arom-C); MS (80 eV, EI, 240 °C): *m*/*z* (%): 622 (5.6) $[M]^+$, 440 (100) $[M-C_{14}H_{10}]^+$, 365 (62.4) $[M-C_{14}H_{10}-Br]^+$ 178 (69.4) $[C_{14}H_{10}]^+$; elemental analysis calcd (%) for $C_{34}H_{38}Br_2O$ (622.47): C 65.60, H 6.15; found: C 65.89, H 6.29.

endo-***14***: ^{1}H NMR: δ = 0.91 (t, ^3J = 6.6 Hz, 6H; CH_3), 1.2–1.6 (m, 16H; alkyl-CH_2), 2.48 (t, ^3J = 7.7 Hz, 4H; α-CH_2), 3.27 (m, AA′BB′, 4H; H-1,2), 4.65 (m, ^3J = 3.4 Hz, 2H; H-4b,10a), 5.73 (m, ^3J = 3.4 Hz, 2H; H-5,10), 7.00 (d, ^3J = 6.9 Hz, 2H; H-3,12), 7.14 ppm (d, ^3J = 6.9 Hz, 2H; H-4,11); ^{13}C NMR (125 MHz): δ = 14.13, 22.63, 28.81, 29.53, 31.38, 31.62, 35.22 (alkyl-C and C-1,2), 54.11 (C-4b,10a), 80.85 (C-5,10), 119.80, 120.76, 125.27, 134.41, 135.71, 138.09, 139.51, 14.72, 142.51 (arom-C); MS (80 eV, EI, 210 °C): *m*/*z* (%): 622 (6.8) $[M]^+$, 444 (100) $[M-C_{14}H_{10}]^+$, 365 (52) $[M-$

$C_{14}H_{10}-Br]^+$ 178 (51) $[C_{14}H_{10}]^+$; elemental analysis calcd (%) for $C_{34}H_{38}Br_2O$ (622.47): C 65.60, H 6.15; found: C 65.56, H 6.13.

4b,5,10,10a-Tetrahydro-7,8-dibromo-5,10-epoxy-6,9-dihexylbenzo[*k*]cyclopenta[*c*,*d*]fluoranthene (15):

*endo-**15***: DDQ (3.2 g, 14 mmol) was added to a refluxing solution of *endo*-**14** (8.6 g, 13.8 mmol) in toluene (150 mL). After refluxing for 90 min, the solution was allowed to cool for 15 min and was then concentrated to a volume of 80 mL in vacuo. The product was isolated from this solution by column chromatography (silica gel, toluene) as 7.3 g of a yellow solid (R_f = 0.54) in 85% yield; ^{1}H NMR: δ = 0.96 (t, ^3J = 6.5 Hz, 6H; CH_3), 1.2–1.6 (m, 16H; alkyl-CH_2), 2.54 (t, ^3J = 7.6 Hz, 4H; α-CH_2), 4.71 (m, ^4J = 3.7 Hz, 2H; H-4b,10a), 5,74 (m, ^4J = 3.7 Hz, 2H; H-5,10), 6.96 (s, 2H; H-1,2), 7.27 (d, ^3J = 6.9 Hz, 2H; H-4,11), 7.51 ppm (d, ^3J = 6.9 Hz, 2H; H-3,12); ^{13}C NMR: δ = 14.10, 22.63, 28.85, 29.53, 31.64, 35.30 (alkyl-C), 54.96 (C-4b,10a), 80.32 (C-5,10), 120.83, 125.27, 125.68, 127.16, 129.00, 134.45, 136.55, 136.67, 141.23, 141.45 ppm (arom-C and C-1,2); MS (80 eV, EI, 130 °C): *m*/*z* (%): 620 (5.6) $[M]^+$, 444 (71.6) $[M-C_{14}H_8]^+$, 365 (100) $[M-C_{14}H_8-Br]^+$; elemental analysis calcd (%) for $C_{34}H_{36}Br_2O$ (620.46): C 65.82, H 5.85; found: C 65.94, H 5.62.

*exo-**15***: Prepared from *exo*-**14** (2.12 g, 3.4 mmol) by a procedure similar to that described above to give 1.52 g of a yellow solid in 72% yield (R_f = 0.72, m.p. 152–154 °C); ^{1}H NMR: δ = 0.97 (t, ^3J = 6.9 Hz, 6H; CH_3), 1.38 (m, 12H; alkyl-CH_2), 1.62 (m, 4H; β-CH_2), 2.95 (m, 4H; α-CH_2), 3.97 (s, 2H; H-4b,10a), 5.43 (s, 2H; H-5,10), 7.14 (s, 2H; H-1,2), 7.52 (d, 2H, ^3J = 6.86 Hz, H-3,12), 7.79 ppm (d, 2H, ^3J = 6.86 Hz, H-4,11); ^{13}C NMR (125 MHz): δ = 14.13, 22.61, 29.47, 29.49, 31.57, 35.13 (alkyl-C), 55.92 (C-4b,10a), 82.53 (C-5,10), 120.73, 126.15, 126.35, 126.95, 129.16, 134.48, 136.64, 137.10, 143.72, 144.12 ppm (arom-C); MS (80 eV, EI, 230 °C): *m*/*z* (%): 620 (1.9) $[M]^+$, 444 (38.2) $[M-C_{14}H_8]^+$, 365 (33) $[M-C_{14}H_8-Br]^+$, 176 (100) $[C_{14}H_8]^+$; elemental analysis calcd (%) for $C_{34}H_{36}Br_2O$ (620.46): C 65.82, H 5.85; found: C 65.66, H 5.80.

4b,5,7,10,12,12a-Hexahydro-5,12,7,10-diepoxy-6,11-dihexylcyclopenta[*c*,*d*]naphtho[2,3-*k*]fluoranthene (16):

***endo-syn*-16 and *endo-anti*-16**: A solution of *endo*-**15** (5.44 g, 8.8 mmol) in dry toluene (350 mL) and dry furan (30 mL) was prepared under nitrogen. This solution was cooled to −30 °C and 6 mL of a 1.6 M solution of BuLi were added dropwise over a period of 1 h. The solution was stirred for an additional 2 h at −30 °C. The reaction was quenched by adding water (5 mL). After warming to room temperature, the volume of the mixture was reduced to 30 mL in a vacuum. This solution was subjected to chromatography (silica gel, toluene) to give the mixture of isomers as a yellow oil (R_f = 0.28). The *syn*/*anti* ratio was 1:1.5 by ^{1}H NMR spectroscopy. The isomers were separated by column chromatography (silica gel, hexane/methylene chloride 2:1) to yield 930 mg of *endo-anti*-**16** (R_f = 0.23) as a yellow oil and 1.53 g *endo-syn*-**16** (R_f = 0.17) as a yellow solid (m.p. 91–93 °C) in a total yield of 53%.

*endo-syn-**16***: ^{1}H NMR (500 MHz): δ = 0.91 (t, ^3J = 6.9 Hz, 6H; CH_3), 1.35 (m, 16H; alkyl-CH_2), 2.00 (m, 2H; α-CH_2), 2.33 (m, 2H; α-CH_2), 4.63 (m, ^4J = 4.2 Hz, 2H; H-4b,12a), 5.28 (s, 2H; H-7,10), 5.68 (m, ^4J = 4.6 Hz, 2H; H-5,12), 6.08 (s, 2H; H-8,9), 6.89 (s, 2H; H-1,2), 7.18 (d, ^3J = 6.9 Hz, 2H; H-4,13), 7.39 ppm (d, ^3J = 6.9 Hz, 2H; H-3,14); ^{13}C NMR (125 MHz, $CDCl_3$): δ = 14.08, 22.56, 29.34, 30.72, 30.83, 31.68 (alkyl-C), 55.01 (C-4b,12a), 80.02 (C-5,12 or C-7,10), 80.71 (C-7,10 or C-5,12), 120.23, 124.42, 125.88, 128.44, 135.89, 136.01, 138.27, 141.29, 142.59, 146.55 ppm; MS (80 eV, EI, 190 °C): *m*/*z* (%): 528 (1.84) $[M]^+$, 352 (100) $[M-C_{14}H_8]^+$, 176 (14.81) $[C_{14}H_8]^+$; HRMS calcd for $C_{38}H_{40}O_2$: 528.302831; found: 528.30395.

*endo-anti-**16***: ^{1}H NMR (500 MHz, CDCl3): δ = 0.90(t, ^3J = 6.8 Hz, 6H; CH_3), 1.28 (m, 14H; alkyl-CH_2), 1.44 (m, 2H; β-CH_2), 2.26 (m, 2H; α-CH_2), 2.40 (m, 2H; α-CH_2), 4.67 (m, ^4J = 4.3 Hz, 2H; H-4b,12a), 5.33 (s, 2H; H-7,10), 5.68 (m, ^4J = 4.3 Hz, 2H; H-5,12), 6.79 (s, 2H; H-8,9), 6.92 (s, 2H; H-1,2), 7.25 (d, ^3J = 6.8 Hz, 2H; H-4,13), 7.48 ppm (d, 2H, ^3J = 6.8 Hz; H-3,14); ^{13}C NMR (125 MHz, $CDCl_3$): δ = 14.09, 22.56, 29.33, 30.27, 31.06, 31.69 (alkyl-C), 54.94 (C-4b,12a), 79.57 (C-5,12 or C-7,10), 80.49 (C-7,10 or C-5,12), 120.37, 125.04, 125.77, 127.05, 128.05, 136.39, 136.71, 138.74, 142.21, 143.02, 146.06 ppm; MS (80 eV, EI, 215 °C): *m*/*z* (%): 528 (4.67) $[M]^+$, 352 (100) $[M-C_{14}H_8]^+$, 176 (14) $[C_{14}H_8]^+$; HRMS calcd for $C_{38}H_{40}O_2$: 528.302831; found: 528.30420.

***exo-syn*-16 *and exo-anti*-16**: The procedure was similar to that used for *endo-syn*-**16** and *endo-anti*-**16** starting from *exo*-**15** (1.73 g, 3.3 mmol). The isomers were separated by column chromatography (silica gel, CH_2Cl_2) to give 424 mg of *exo-syn*-**16** (R_f = 0.15) and 457 mg of *exo-anti*-**16** (R_f = 0.27) in a total yield of 50%.

*exo-anti-**16***: ^{1}H NMR (500 MHz, $CDCl_3$): δ = 0.95 (t, 6H, ^3J = 6.7 Hz; CH_3), 1.45 (m, 14H; alkyl-CH_2), 1.67 (m, 2H; β-CH_2), 2.71 (m, 2H; α-CH2), 2.81 (m, 2H; α-CH2), 3.95 (s, 2H; H-4b,12a), 5.38 (s, 2H; H-7,10), 5.83 (s, 2H; H-5,12), 7.03 (s, 2H; H-8,9), 7.13 (s, 2H; H-1,2), 7.51 (d, ^3J = 6.8 Hz, 2H; H-4,13), 7.78 ppm (d, ^3J = 6.8 Hz, 2H; H-3,14); ^{13}C NMR (125 MHz, $CDCl_3$): δ = 14.15, 22.60, 29.28, 30.24, 31.39, 31.71 (alkyl-C), 56.12 (C-4b,12a), 81.04 (C-5,12 or C-7,10), 81.87 (C-7,10 or C-5,12), 120.62, 126.08, 126.95, 129.04, 136.46, 137.21, 142.14, 142.92, 144.42, 147.15 ppm (arom-C); MS (80 eV, EI, 220 °C): *m*/*z* (%): 528 (1.65) $[M]^+$, 352 (100) $[M-C_{14}H_8]^+$, 176 (9.52) $[C_{14}H_8]^+$; HRMS calcd for $C_{38}H_{40}O_2$: 528.302831; found: 528.30475.

*exo-syn-**16***: ^{1}H NMR (500 MHz, $CDCl_3$): δ = 0.96 (t, 6H, ^3J = 6.7 Hz, CH_3), 1.42 (m, 12H; alkyl-CH_2), 1.68 (m, 4H; β-CH_2), 2.79 (m, 4H; α-CH_2), 3.99 (s, 2H; H-4b,12a), 5.40 (s, 2H; H-7,10), 5.82 (s, 2H; H-5,12), 7.12 (s, 2H; H-8,9), 7.15 (s, 2H; H-1,2), 7.54 (d, ^3J = 6.8 Hz, 2H; H-4,13), 7.80 ppm (d, 2H, ^3J = 6.8 Hz; H-3,14); ^{13}C NMR (125 MHz, $CDCl_3$): δ = 14.11, 22.58, 29.27, 30.21, 31.15, 31.77 (alkyl-C), 56.34 (C-4b,12a), 81.12 (C-5,12 or C-7,10), 81.95 (C-7,10 or C-5,12), 120.41, 125.82, 126.07, 126.95, 129.02, 136.42, 137.39, 142.17, 144.42, 143.05, 147.63 ppm; MS (80 eV): *m*/*z* (%): 528 (2.92) $[M]^+$, 352 (100) $[M-C_{14}H_8]^+$, 176 (17.79) $[C_{14}H_8]^+$; HRMS calcd for $C_{38}H_{40}O_2$: 528.302831; found: 528.30646

4b,5,7,7a,8,11,11a,12,14,14a-Decahydro-8,11-carbonyl-5,14:7,12-diepoxy-6,13-dihexyl-8,9,10,11-tetraphenylacenaphtheno[1′,8′:2,3,4]cyclopenta[1,2-*b*]naphthacene (17): As a representative procedure for the synthesis of the four isomers of **17**, the one for *endo-anti*-**17** is given. A suspension of *endo-anti*-**16** (830 mg, 1.57 mmol) and tetracyclone (604 mg, 1.57 mmol) in ethanol (100 mL) was refluxed for 2 h under nitrogen atmosphere. The mixture was dried in vacuum and the residue purified by column chromatography (silica gel, toluene) to give a pale yellow solid (R_f = 0.38). Yield: 960 mg (67%); m.p. 187–189 °C (decomp.); ^{1}H NMR (500 MHz, $CDCl_3$): δ = 0.97 (t, 6H, ^3J = 6.8 Hz; CH_3), 1.40 (m, 8H; alkyl-CH_2), 1.57 (m, 6H; β,γ-CH_2), 1.69 (m, 2H; β-CH_2), 2.48 (m, 2H; α-CH_2), 2.61 (m, 2H; α-CH_2), 2.82 (s, 2H; H-7a,11a), 4.75 (m, ^4J = 3.7 Hz, 2H; H-4b,14a), 5.45 (s, 2H; H-7,12), 5.80 (m, ^4J = 3.7 Hz, 2H; H-5,14), 6.73 (m, 4H; phenyl-H), 6.89 (m, 4H; phenyl-H), 6.93 (s, 2H; H-1,2), 6.96 (m, 2H; phenyl-H), 7,30 (m, 8H; phenyl-H), 7.35 (m, 4H; phenyl-H and H-4,15), 7.51 ppm (d, ^3J = 6.9 Hz, 2H, H-3–16); ^{13}C NMR (125 MHz, $CDCl_3$): δ = 14.15, 22.76, 29.66, 30.25, 31.10, 31.46 (alkyl-C), 46.94 (C-7a,11a), 54.97 (C-4b,14a), 64.06 (C-8,11), 79.51 (C-5,14 or C-7,12), 79.59 (C-7,12 or C-5,14), 120.47, 124.54, 125.18, 126.55, 127.16, 127.25, 127.37, 128.10, 128.90, 129.31, 129.76, 134.97, 135.64, 136.53, 136.78, 138.27, 140.79, 142.99, 143.90 (arom-C and C-1,2), 196.52 ppm (carbonyl-C); MS (FAB$^+$): *m*/*z* (%): 913 (0.2) $[M+H]^+$.

***endo-syn*-17**: Yellow crystals (R_f (CH_2Cl_2) = 0.43); yield: 1.42 g (54%) along with 664 mg (18%) of the colorless bisadduct. Single crystals of *endo-syn*-**17** for X-ray crystallographic analysis were obtained by recrystallization from ethanol. ^{1}H NMR (500 MHz, $CDCl_3$): δ = 0.88 (t, ^3J = 6.6 Hz, 6H; CH_3), 1.23 (s, 2H; H-7a,11a), 1.32 (m, 8H; alkyl-CH_2), 1.40 (m, 4H; γ-CH_2), 1.62 (m, 4H; β-CH_2), 2.17 (m, 2H; α-CH_2), 2.51 (m, 2H; α-CH_2), 4.73 (m, ^4J = 3.9 Hz, 2H; H-4b,14a), 5.28 (s, 2H; H-7,12), 5.80 (m, ^4J = 3.9 Hz, 2H, H-5,14), 6.19 (s, 2H; H-1,2), 6.77 (m, 4H; phenyl-H), 6.91 (m, 4H), 6.97 (m, 2H), 7.22 (m, 6H), 7.27 (m, 2H), 7.36 (m, 2H), 7.43 ppm (m, 4H; phenyl-H and H-3,4,15,16); ^{13}C NMR (125 MHz, $CDCl_3$): δ = 14.10, 22.48, 28.97, 30.89, 31.53, 31.76 (alkyl-C), 46.00 (C-7a,11a), 55.12 (C-4b,14a), 63.75 (C-8,11), 79.62 (C-5,14 or C-7,12), 80.17 (C-7,12 or C-5,14), 120.47, 124.15, 124.37, 125.92, 126.50, 127.04, 127.36, 127.95, 129.18, 129.34, 129.70, 135.00, 135.44, 135.52, 136.34, 138.26, 140.70, 142.66, 144.75 (arom-C and C-1,2), 195.31 ppm (carbonyl-C); MS (FAB$^+$): *m*/*z* (%): 913 (2) $[M+H]^+$; elemental analysis calcd (%) for $C_{67}H_{60}O_3$ (913.19): C 88.12, H 6.62; found: C 87.82, H 6.68.

1,4,4a,6b,7,9,9a,10,13,13a,14,16,16a,18b-Tetradecahydro-1,4:10,13-dicarbonyl-7,16:9,14-diepoxy-8,15-dihexyl-1,2,3,4,10,11,12,13-octaphenyl-fluoranthreno[3′,4′:2,3,4]cyclopenta[1,2-*b*]naphthacene (bisadduct): ^{1}H NMR: δ = 0.90 (t, ^3J 6.4 Hz, 6H; CH_3), 1.36 (m, 12H; CH_2), 1.57 (s, 2H; H-9a,13a), 1.64 (m, 4H; β-CH_2), 2.12 (m, 2H; α-CH_2), 2.48 (m, 2H; α-CH_2), 3.79 (m, 2H; H-6a,16a), 4.03 (s, 2H; H-4a,18b), 5.40 (s, 2H; H-9,14), 5.73 (m, 2H; H-7,16), 5,97 (d, ^3J = 7 Hz, 2H; H-5,18 or H-6,17), 6.61 (d, ^3J = 7 Hz, 2H;

H-5,18 or H-6,17), 6.78 (m, 4H; phenyl-H), 7.10 (m, 26H; phenyl-H), 7.49 ppm (m, 10H; phenyl-H); ^{13}C NMR: $\delta = 14.04$, 22.44, 28.95, 30.81, 31.50, 31.64 (alkyl-C), 46.27 (C-9a,13a), 53.81 (C-4a,18b or C-6b,16a), 55.78 (C-4a,18b or C-6b,16a), 63.48 (C-1,4 or C-10,13), 64.14 (C-1,4 or C-10,13), 79.91 (C-7,16 or C-9,14), 80.40 (C-7,16 or C-9,14), 120.43, 122.61, 124.16, 126.26, 126.33, 126.79, 126.98, 127.10, 127.56, 128.25, 129.58, 129.76, 129.93, 134.66, 134.74, 134.83, 135.37, 136.02, 138.20, 138.51, 138.93, 141.39, 144.23, 145.08, 197.06 (carbonyl-C), 201.94 ppm (carbonyl-C); MS (FAB)$^+$: *m*/*z* (%): 1298 (1.5) $[M+H]^+$.

*exo-anti-**17***: Pale yellow solid; yield: 376 mg (67%); ^{1}H NMR (500 MHz, $CDCl_3$): $\delta = 0.93$ (t, 6H, $^3J = 7.1$ Hz; CH_3), 1.44 (m, 8H; CH_2), 1.63 (m, 4H; γ-CH_2), 1.83 (m, 4H; β-CH_2), 2.91 (m, 2H; α-CH_2), 2.96 (m, 2H; α-CH_2), 3.07 (s, 2H; H-7a,11a), 3.98 (s, 2H; H-4b,14a), 5.50 (s, 2H; H-7,12), 5.90 (s, 2H; H-5,14), 6.91 (m, 4H; phenyl-H), 6.98 (m, 6H; phenyl-H), 7.15 (s, 2H; H-1,2), 7.33 (m, 2H; phenyl-H), 7.40 (m, 4H; phenyl-H), 7.48 (m, 4H; phenyl-H), 7.56 (d, $^3J = 6.7$ Hz, 2H; H-4,15), 7.80 ppm (d, $^3J = 6.7$ Hz, 2H; H-3,16); ^{13}C NMR (125 MHz): $\delta = 14.03$, 22.58, 29.64, 30.83, 31.56, 31.61 (alkyl-C), 46.57 (C-7a,11a), 55.97 (C-4b,14a), 64.11 (C-8,11), 81.65 (C-5,14 or C-7,12), 82.58 (C-7,12 or C-5,14), 120.56, 124.57, 125.99, 126.59, 126.86, 127.29, 127.39, 128.17, 128.98, 129.27, 129.78, 135.01, 135.38, 136.43, 137.12, 138.43, 143.73, 144.06, 144.80 (arom-C and C-1,2), 196.39 ppm (carbonyl-C); MS (FAB$^+$): *m*/*z* (%): 913 (1) $[M+H]^+$.

*exo-syn-**17***: Pale yellow solid; yield: 501 mg (75%); ^{1}H NMR (500 MHz, $CDCl_3$): $\delta = 0.99$ (t, 6H, $^3J = 7.2$ Hz; CH_3), 1.48 (m, 8H; alkyl-CH_2), 1.66 (m, 4H; γ-CH_2), 1.83 (m, 4H; β-CH_2), 2.91 (m, 2H; α-CH_2), 3.01 (m, 2H; α-CH_2), 3.20 (s, 2H; H-7a,11a), 4.06 (s, 2H; H-4b,14a), 5.46 (s, 2H; H-7,12), 5.89 (s, 2H; H-5,14), 6.92 (m, 4H; phenyl-H), 7.01 (m, 6H; phenyl-H), 7.14 (s, 2H; H-1,2), 7.33 (m, 2H; phenyl-H), 7.40 (m, 4H; phenyl-H), 7.51 (m, 4H; phenyl-H), 7.54 (d, $^3J = 6.8$ Hz, 2H; H-4,15), 7.80 ppm (d, $^3J = 6.8$ Hz, 2H; H-3,16); ^{13}C NMR (125 MHz): $\delta = 14.14$, 22.68, 28.88, 31.21, 31.70, 31.77 (alkyl-C), 47.05 (C-7a,11a), 56.35 (C-4b,14a), 64.30 (C-8,11), 80.21 (C-5,14 or C-7,12), 81.98 (C-7,12 or C-5,14), 120.59, 124.62, 126.14, 126.73, 127.05, 127.38, 127.53, 128.24, 129.11, 129.46, 129.91, 135.14, 135.72, 136.61, 137.26, 138.54, 144.01, 144.40, 144.99 (arom-C and C-1,2), 196.79 ppm (carbonyl-C); MS (FAB$^+$): *m*/*z* (%): 913 (3) $[M+H]^+$; elemental analysis calcd (%) for $C_{67}H_{60}O_3$ (913.19): C 88.12, H 6.62; found: C 88.36, H 6.33.

***rel*-(1*R*,4*S*,4a*S*,6b*S*,7*R*,9*S*,9a*S*,11b*S*,12*R*,15*S*,15a*R*,17b*R*,18*R*,20-*S*,20a*R*,22b*R*)-1,4:7,20:9,18:12,15-Tetraepoxy-8,19,23,24-tetrahexyl-1,4,4a,6b,7,9,9a,11b,12,15,15a,17b,18,20,20a,22b-hexadecahydro-2,14:3,13-dimethenodiindeno[1,2,3-*c*,*d*:1′,2′,3′-*c*′,*d*′]benzo[2,3-*j*:5,6-*j*′]difluoranthene (19)**: Typical procedure: A solution of *exo-syn*-**19** (230 mg, 0.25 mmol) in toluene (10 mL) was prepared under nitrogen and refluxed for 2 d. After cooling to room temperature and removal of solvent in vacuo, the residue was purified by column chromatography (CH_2Cl_2) to afford a colorless solid (m.p. 286–287 °C, decomp) in 43% yield ($R_f = 0.25$). Single crystals were grown by diffusion of ethanol into a chloroform solution. ^{1}H NMR: $\delta = 0.88$ (t, $^3J = 6.4$ Hz, 12H; CH_3), 1.31 (m, 24H; alkyl-CH_2), 1.50 (s, 4H; H-6b,11b,15a,20a), 1.56 (m, 8H; β-CH_2), 2.00 (m, 4H; α-CH_2), 2.34 (m, 4H; α-CH_2), 4.71 (m, $^4J = 3.7$ Hz, 4H; H-4a,9a,17b,22b), 5.13 (s, 4H; H-7,12,15,20), 5.73 (m, $^4J = 3.7$ Hz, 4H; H-1,4,9,18), 7.03 (d, $^3J = 6.9$ Hz, 4H; H-5,10,17,21 or H-6,11,16,22), 7.19 ppm (d, $^3J = 6.9$ Hz, 4H; H-5,10,17,21 or H-6,11,16,22); ^{1}H NMR ([D$_6$]benzene): $\delta = 0.89$ (t, $^3J = 6.6$ Hz, 12H; CH_3), 1.22 (m, 16H; alkyl-CH_2), 1.35 (m, 8H; γ-CH_2), 1.50 (m, 8H; α-CH_2), 1.65 (s, 4H; H-6b,11b,15a,20a), 2.03 (m, 4H; α-CH_2), 2.28 (m, 4H; α-CH_2), 4.54 (m, $^4J = 3.7$ Hz, 4H; H-4a,9a,17b,22b), 5.34 (s, 4H; H-7,12,15,20), 5.68 (m, $^4J = 3.7$ Hz, 4H; H-1,4,9,18), 6.77 (d, $^3J = 6.9$ Hz, 4H; H-5,10,17,21 or H-6,11,16,22), 6.87 (d, $^3J = 6.9$ Hz, 4H; H-5,10,17,21 or H-6,11,16,22); ^{13}C NMR (125 MHz): $\delta = 14.10$, 22.54, 29.19, 31.15, 31.70, 31.75 (alkyl-*C*), 54.69 (C-4a,9a,17a,22b), 57.23 (C-6b,11b,15a,17a), 80.60 (C-1,4,9,18), 81.56 (C-7,12,15,20), 120.21, 121.16, 125.29, 138.62, 139.39, 139.60, 140.67, 141.80, 144.05 ppm (arom-C); MS (80 eV, EI, 140 °C): *m*/*z* (%): 1004 (1.8) $[M]^+$, 828 (0.9) $[M - C_{14}H_8]^+$, 502 (18) $[M - C_{36}H_{38}O_2]^+$, 326 (100) $[M - C_{36}H_{38}O_2 - C_{14}H_8]^+$; elemental analysis calcd (%) for $C_{72}H_{76}O_4$ (1005.33): C 86.02, H 7.62; found: C 85.78, H 7.58.

6a,7,12,12a-Tetrahydro-7,12-epoxybenzo[*k*]fluoranthene (22): A solution of acenaphthylene (4.77 g, 31 mmol) and of the isobenzofuran precursor **21**[20] (16.4 g, 31 mmol) in toluene (250 mL) was refluxed for 16 h. After cooling to room temperature, the solvent was evaporated in vacuo. The residue was digested in hot ethanol (250 mL) for 30 min and filtered while hot; this was repeated once. This procedure removed most of the tetraphenylbenzene byproduct. The combined filtrates were dried in vacuo. The isomers were purified and separated by column chromatography (silica, hexane/ethyl acetate 3:1) to give 5.87 g of *endo*-**22** (m.p. 190–191 °C, $R_f = 0.37$) and 1.42 g of *exo*-**22** (m.p. 166–167 °C, $R_f = 0.43$) in an overall yield of 87% as colorless solids. Single crystals for X-ray crystallographic analysis were grown from ethanol.

*endo-**22***: ^{1}H NMR: $\delta = 4.64$ (m, $^3J = 4.0$ Hz, 2H; H-6b,12a), 5.71 (m, 2H, $^4J = 4.0$ Hz, 2H; H-7,12), 6.59 (AA′BB′, 2H; H-8,11 or H-9,10), 6.68 (AA′BB′, 2H; H-8,11 or H-9,10), 7.19 (d, $^3J = 6.6$ Hz, 4H; H-1,6), 7.29 (dd, $^3J = 6.6$ Hz, $^3J = 8.0$ Hz, 2H; H-2,5), 7.37 ppm (d, $^3J = 8.0$ Hz, 2H; H-3,4); ^{13}C NMR: $\delta = 52.05$ (C-6b,12a), 81.73 (C-7,12), 119.29, 120.35, 123.09, 125.52, 127.24, 131.21, 142.18, 142.27 ppm (arom-C); MS (80 eV, EI, 80 °C): *m*/*z* (%): 270 (76) $[M]^+$, 252 (26) $[M - H_2O]^+$, 152 (5) $[C_{12}H_8]^+$, 118 (100) $[M - C_{12}H_8]^+$; elemental analysis calcd (%) for $C_{20}H_{14}O$ (270.32): C 88.86, H 5.22; found: C 88.80, H 5.11.

*exo-**22***: ^{1}H NMR: $\delta = 3.93$ (s, 2H; H-6b,12a), 5.48 (s, 2H; H-7,12), 7.29 (AA′BB′, 2H; H-8,11 or H-9,10), 7.46 (AA′BB′; 2H, H-8,11 or H-9,10), 7.56 (m, 4H; H-1,6 and H-2,5), 7.74 ppm (d, $^3J = 7.8$ Hz, 2H; H-3,4); ^{13}C NMR: $\delta = 53.28$ (C-6b,12a), 84.30 (C-7,12), 119.49, 119.53, 123.54, 126.94, 127.96, 131.37, 143.95, 145.87 ppm (arom-C); MS (80 eV, EI, 130 °C): *m*/*z* (%): 270 (18) $[M]^+$, 252 (3) $[M - H_2O]^+$, 152 (12) $[C_{12}H_8]^+$, 118 (100) $[M - C_{12}H_8]^+$; elemental analysis calcd (%) for $C_{20}H_{14}O$ (270.32): C 88.86, H 5.22; found: C 88.83, H 5.29.

***rel*-(1*R*,4*S*,4a*S*,9*S*,9a*S*,17b*R*,18*R*,22b*R*)-1,4:9,18-Diepoxy-8,19,23,24-tetrahexyl-1,4,4a,9,9a,17b,18,22b-octahydro-2,14:3,13-dimethenodiindeno[1,2,3-*c*,*d*:1′,2′,3′-*c*′,*d*′]benzo[2,3-*j*:5,6-*j*′]difluoranthene (23)**: A solution of **19** (60 mg, 0.06 mmol) in toluene (5 mL) was prepared under nitrogen atmosphere and heated to reflux. *p*-TosH monohydrate (45 mg) was added and the mixture was refluxed for 16 h. After cooling to room temperature, the solution was washed three times with water and the organic layer was dried in vacuo. The residue was purified by column chromatography (silica gel, CH_2Cl_2)to give 27 mg of a pale yellow green solid (m.p. >310 °C) in 47% yield. Single crystals for X-ray crystallographic analysis were grown by the diffusion of hexane into a solution of **23** in chloroform; ^{1}H NMR: $\delta = 0.87$ (t, $^3J = 6.3$ Hz, 12H; CH_3), 1.1–1.5 (m, 24H; alkyl-CH_2), 1.58 (m, 8H; β-CH_2), 2.49 (m, 4H; α-CH_2), 2.74 (m, 4H; α-CH_2), 4.77 (m, $^4J = 3.9$ Hz, 4H; H-4a,9a,17b,22b), 5.92 (m, $^4J = 3.9$ Hz, 4H; H-1,4,9,18), 7.26 (d, $^3J = 6.9$ Hz, 4H; H-5,10,17,21 or H-6,11,16,22), 7.47 (s, 4H; H-7,12,15,20), 7.49 ppm (d, $^3J = 6.9$ Hz, 4H, H-5,10,17,21 or H-6,11,16,22); ^{13}C NMR (125 MHz): $\delta = 14.11$, 22.61, 29.58, 30.93, 31.52, 31.76 (alkyl-C), 55.91 (C-4a,9a,17a,22b), 81.66 (C-1,4,9,18), 116.25, 119.39, 121.43, 128.87, 131.00, 133.49, 134.47, 136.28, 137.24, 137.44, 142.31 ppm (arom-C); MS (80 eV, EI, 260 °C): *m*/*z* (%): 968 (38) $[M]^+$, 484 (100) $[M - C_{36}H_{36}O$ or $M]^{2+}$, 413 (19) $[M - C_{36}H_{36}O - C_5H_{11}]^+$.

Acknowledgement

We thank the Fonds der Chemischen Industrie for financial support of this work.

[1] a) A. D. Schlüter, *Adv. Mater.* **1991**, *3*, 282–291; b) "Synthesis of Polymers": A. D. Schlüter, *Material Science and Technology Series*, Wiley-VCH Weinheim, **1999**, pp. 459–484

[2] a) A. Godt, V. Enkelmann, A. D. Schlüter, *Angew. Chem.* **1989**, *101*, 1704–1706; *Angew. Chem. Int. Ed. Engl.* **1989**, *28*, 1680–1682; b) O. Kintzel, A. D. Schlüter, *Acta Polymer.* **1997**, *48*, 212–214; c) O. Kintzel, P. Luger, M. Weber, A. D. Schlüter, *Eur. J. Org. Chem.* **1998**, 99–105.

[3] a) P. R. Ashton, G. R. Brown, N. S. Isaacs, D. Giuffrida, F. H. Kohnke, J. P. Mathias, A. M. Z. Slawin, D. R. Smith, J. F. Stoddart, D. J. Williams, *J. Am. Chem. Soc.* **1992**, *114*, 6330–6353; b) J. Benkhoff, R. Boese, F.-G. Klärner, A. E. Wigger, *Tetrahedron Lett.* **1994**, *35*, 73–76; c) R. M. Cory, C. L. McPhail, *Tetrahedron Lett.* **1996**, *37*, 1987–1990; d) R. M. Cory, C. L. McPhail, *Tetrahedron Lett.* **1996**, *37*, 1983–1986; e) F. Vögle, *Top. Curr. Chem.* **1983**, *115*, 153–157.

[4] J.-I. Aihara, *J. Chem. Soc. Perkin Trans. 2* **1994**, 971–974.

[5] a) H. S. Choi, K. S. Kim, *Angew. Chem.* **1999**, *111*, 2400–2402; *Angew. Chem. Int. Ed.* **1999**, *38*, 2256–2258; b) K. N. Houk, P. S. Lee, M. Nendel, *J. Org. Chem.* **2001**, *66*, 5517–5521

[6] a) Y. Kuwatani, paper presented at the *10th International Symposium on Novel Aromatics*, San Diego, **2001**; b) G. J. Bodwell, D. O. Miller, R. J. Vermeij, *Org. Lett.* **2001**, *3*, 2093–2096.
[7] a) A. D. Schlüter, M. Löffler, V. Enkelmann, *Nature* **1994**, *368*, 831–834; b) M. Löffler, A. D. Schlüter, K. Geßler, W. Saenger, J.-M. Toussaint, J.-L. Bredas, *Angew. Chem.* **1994**, *106*, 2281–2284; *Angew. Chem. Int. Ed. Engl.* **1994**, *33*, 2209–2212; c) B. Schlicke, H. Schirmer, A. D. Schlüter, *Adv. Mater.* **1995**, *7*, 544–546.
[8] M. M. Boorum, Y. V. Vasiliev, T. Drewello, L. T. Scott, *Science* **2001**, *294*, 828–834, and references therein.
[9] a) T. Sasaki, K. Kanematsu, K. Iizuka, *J. Org. Chem.* **1976**, *41*, 1105–1112; b) S. Mondal, T. K. Bandyopadhyay, A. J. Bhattacharya, *Ind. J. Chem.* **1983**, *22*, 225–229.
[10] a) K. Harano, M. Yasuda, K. Kanematsu, *J. Org. Chem.* **1982**, *47*, 3736–3743; b) W. Ried, R. Neidhardt, *Liebigs Ann. Chem.* **1970**, *739*, 155–158; c) V. V. Plemenkov, L. A. Yanykina, *J. Org. Chem. USSR (Engl. Transl.)* **1970**, *6*, 2049–2052.
[11] a) A. G. Anderson, R. G. Anderson, *J. Org. Chem.* **1958**, *23*, 517–520; b) H.-J. Bestmann, R. Armsen, H. Wagner, *Chem. Ber.* **1969**, *102*, 2259–2269; c) B. M. Trost, G. M. Bright, C. Frihart, D. Britelli, *J. Am. Chem. Soc.* **1971**, *93*, 737–745.
[12] B. M. Trost, D. Buhner, G. M. Bright, *Tetrahedron Lett.* **1973**, *29*, 2787–2790.
[13] N. Tanaka, T. Kasai, *Bull. Chem. Soc. Jpn.* **1981**, *54*, 3020–3023
[14] R. G. Harvey, L. Nazareno, H. Cho, *J. Am. Chem. Soc.* **1973**, *95*, 2376–2378
[15] M. R. Churchill, J. Wormald, *Chem. Commun.* **1968**, 1597–1598.
[16] H. Meier, B. Rose, *Liebigs Ann./Recl.* **1997**, *4*, 663–670.
[17] H. Hart, C.-Y. Lai, G. C. Nwokogu, S. Shamouilian, *Tetrahedron* **1987**, *43*, 5203–5224.
[18] *exo-anti*-**17** could not be obtained in pure form.
[19] T. Vogel, Dissertation, **1990**, University of Mainz (Germany).
[20] R. Packe-Wirth, V. Enkelmann, *J. Mol. Struct.* **1998**, *448*, 1–9, and references therein.
[21] H. Schirmer, A. D. Schlüter, V. Enkelmann, *Chem. Ber.* **1993**, *126*, 2543–2546.
[22] a) G. H. Olah, S. C. Narang, B. G. B. Gupta, R. Mahalta, *Angew. Chem.* **1979**, *91*, 648–649; *Angew. Chem. Int. Ed. Engl.* **1979**, *18*, 612–614; b) G. H. Olah, *J. Org. Chem.* **1979**, *44*, 1247–1251.
[23] M. J. Dewar, E. G. Zoebisch, E. F. Healy, J. J. P. Stewart, *J. Am. Chem. Soc.* **1985**, *107*, 3902–3909.
[24] R. Notario, J.-L. Abboud, *J. Phys. Chem. A* **1998**, *102*, 5290–5297 and references therein.
[25] a) L. Türker, *THEOCHEM* **2000**, *531*, 333–337; b) L. Türker, *J. Mol. Struct.* **1997**, *407*, 217–220.
[26] M. Kertesz, A. Ashertehrani, *Macromolecules*, **1996**, *29*, 940–945.
[27] W. D. Neudorff, Dissertation, **2002**, Freie Universität Berlin (Germany).
[28] PAs for [*n*]cyclacenes with an even-numbered *n* rise to exceptionally high values (see the Supporting Information). This may be a consequence of the unreliability of the AM1 method for this class of compounds on account of their energetically similar valence-isomeric structures (see ref. [5]).
[29] K. B. Wiberg, *Angew. Chem.* **1986**, *98*, 312–322; *Angew. Chem. Int. Ed. Engl.* **1986**, *25*, 312–322.
[30] "JANAF Thermochemical Tables, 3rd ed.": M. W. Chase, Jr., C. A. Davies, J. R. Downey, D. J. Frurip, R. A. McDonald, A. N. Syverud, *J. Phys. Chem. Ref. Data* **1985**, *14*, (Suppl. 1).
[31] SAINTPLUS Software Reference Manual, Version 5.054, Bruker-AXS, Madison, WI, **1997–1998**.
[32] R. H. Blessing, *Acta Crystallogr. Sect A* **1995**, *51*, 33–38; SADABS, Bruker AXS **1998**.
[33] G. M. Sheldrick, SHELX97 Programs for Crystal Structure Analysis (Release 97–2), University of Göttingen, Göttingen (Germany), **1998**.
[34] PLATON/PLUTON: a) A. L. Spek, *Acta Crystallogr. Sect A* **1990**, *46*, C34; b) A. L. Spek, PLATON, A Multipurpose Crystallographic Tool, Utrecht University, Utrecht (The Netherlands), **1998**.
[35] ORTEP3 for Windows: L. J. Farrugia, *J. Appl. Crystallogr.* **1997**, *30*, 565.
[36] WINGX: L. J. Farrugia, *J. Appl. Crystallogr.* **1999**, *32*, 837–838.
[37] Hypercube, Inc. 1115 NW 4th Street, Gainesville, Florida (USA).

Received: February 6, 2003 [F4824]

